

Optimizing Energy Utilization in the Weaving Industry: Advanced Electrokinetic Solutions with Modified Piezo Matrix and Super Lift Luo Converter

Karthikeyan Saravanan & Johnny Renoald Albert

To cite this article: Karthikeyan Saravanan & Johnny Renoald Albert (09 Oct 2023): Optimizing Energy Utilization in the Weaving Industry: Advanced Electrokinetic Solutions with Modified Piezo Matrix and Super Lift Luo Converter, Electric Power Components and Systems, DOI: [10.1080/15325008.2023.2262458](https://doi.org/10.1080/15325008.2023.2262458)

To link to this article: <https://doi.org/10.1080/15325008.2023.2262458>



Published online: 09 Oct 2023.



Submit your article to this journal [↗](#)



View related articles [↗](#)



View Crossmark data [↗](#)



Optimizing Energy Utilization in the Weaving Industry: Advanced Electrokinetic Solutions with Modified Piezo Matrix and Super Lift Luo Converter

Karthikeyan Saravanan and Johny Renoald Albert

Dept of Electrical and Electronics Engineering Erode, Sengunthar Engineering College, Erode, Tamil Nadu, India

CONTENTS

1. Introduction
2. Background Analysis
3. Summary of Survey
4. Theoretical Frame Work
5. Experimental Source Details Analysis
6. Energy Estimation Verification
7. Future Scope and Implementation
8. Conclusion
9. Future Works for Electro-Kinetic Solutions
- References

Abstract—This project aims to revolutionize energy utilization in the textile industry by optimizing Modified Piezo Matrix-based electro-kinetic energy generation from weaving power looms. It focuses on harnessing kinetic energy from two sources—the open-end head frame and the Weaving X-Y Shuttle box—both generating sequential kinetic energy during weaving. The experimental setup employs a specialized configuration: a 4(4x2) matrix piezo for the open-end head frame and a 2(2x10) matrix piezo for the Weaving X-Y Shuttle box. This arrangement efficiently captures and converts kinetic energy, resulting in remarkable energy outputs of 9.51 Hp and 2.60 Hp for the Open end Head frame and Weaving X-Y shuttle box, respectively. To further enhance energy utilization and integration, a second-level DC-DC power conversion approach is employed, utilizing the Super Lift Luo converter(90% η). This strategy ensures efficient energy transfer and seamless integration with the Industrial DC microgrid. The project's objectives encompass minimizing reliance on fossil fuels, promoting sustainability, and highlighting the potential of electrokinetic solutions for industrial energy optimization. By tapping into previously overlooked kinetic energy sources and maximizing their conversion, this project presents a pioneering effort toward sustainable practices in the textile sector, contributing to environmentally-conscious production methods.

1. INTRODUCTION

The textile industry is a significant consumer of electricity due to its energy-intensive processes and reliance on machinery. From spinning mills to weaving mills and knitting mills, electricity plays a crucial role in powering the various stages of fabric production [1,2]. Spinning mills require substantial electrical power to convert fibers into yarns through spinning processes. Weaving mills use electricity to operate looms and related equipment, while knitting mills rely on electrical power for their knitting machines Figure 1 (Textile Industry Sub-Manual and Non-Manual Processes) [1, 3–5]. Additionally, processes such

Keywords: Textile industry, electrokinetic solutions, energy optimization, modified piezo matrix, super lift luo converter

Received 28 June 2023; accepted 18 September 2023

Address correspondence to Karthikeyan Saravanan, Dept of Electrical and Electronics Engineering Erode, Sengunthar Engineering College, Erode, Tamil Nadu 638057, India. E-mail: karthikeyanthyristorfamily@gmail.com

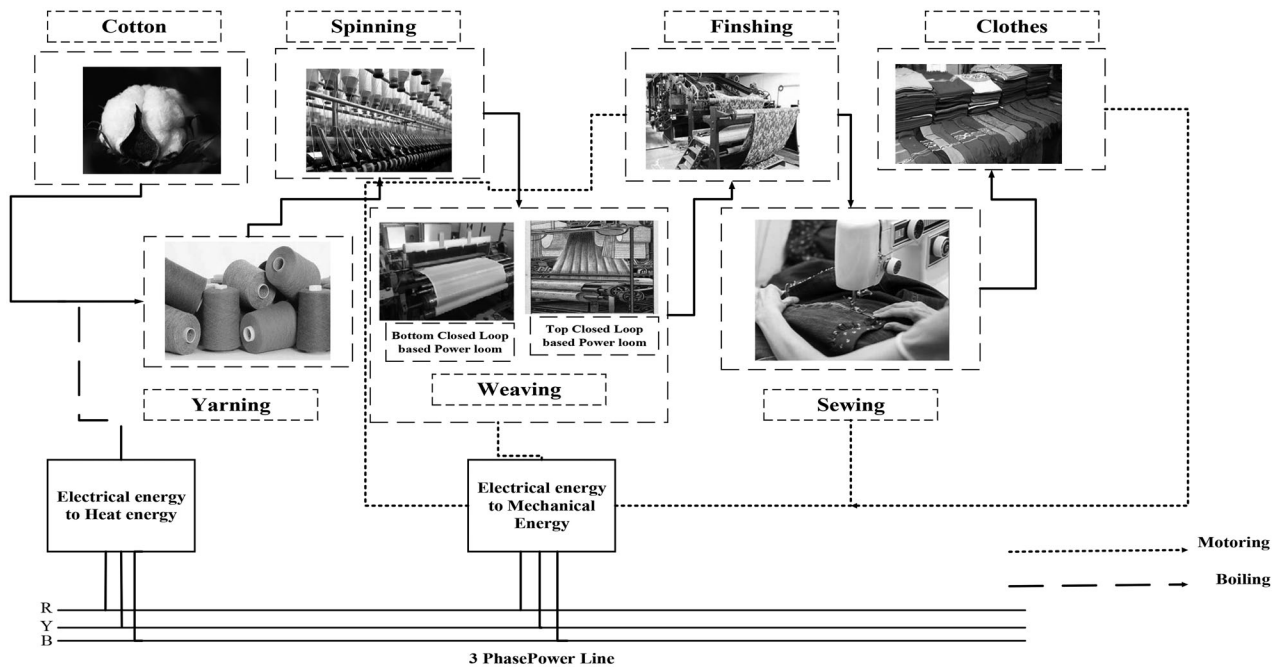


FIGURE 1. Textile industries sub-manual and non-manual process.

as dyeing and printing, finishing, cutting, and sewing also contribute to the industry's electricity demand [6]. Automation and computer-controlled machinery have further increased the electricity requirements in the textile industry. While these advancements have improved production efficiency, they have also led to higher energy consumption per unit of output. Consequently, textile manufacturers are actively seeking ways to enhance energy efficiency and reduce their overall electricity demand. To address the electricity demand, textile industries can implement energy management strategies. Conducting energy audits helps identify areas of electricity waste and suggests improvements. Analyzing energy consumption patterns allows companies to optimize operations and reduce unnecessary energy use [3, 7, 8]. Optimizing the power factor of electrical systems enhances the efficient utilization of electricity, resulting in potential energy and cost savings. Energy management systems and smart grid integration provide real-time monitoring and control of electricity usage, empowering industries to make informed decisions and actively manage their electricity demand. Another avenue for reducing reliance on conventional electricity is the integration of renewable energy sources [4]. Many textile companies are installing solar panels or investing in wind power to generate clean energy [9]. By harnessing renewable sources, textile industries can not only reduce their carbon footprint but also lower their long-term electricity costs [10, 11]. Energy storage systems play a crucial

role in managing electricity demand fluctuations. Textile industries can store excess energy during periods of low demand and utilize it during peak periods, optimizing electricity consumption and reducing strain on the grid [12]. Energy conservation practices also play a vital role in addressing the electricity demand of the textile industry. Simple actions such as turning off equipment when not in use, optimizing production schedules, and minimizing standby power can lead to significant energy savings. Implementing energy-efficient lighting solutions, such as LED technology [9], can substantially reduce electricity demand for lighting requirements. Additionally, the use of variable speed drives in machinery enables optimal electricity consumption by adjusting motor speeds based on load requirements, resulting in energy and cost savings. Managing electricity demand requires consideration of factors such as energy tariffs, load shedding, and peak demand. Understanding different electricity tariffs and pricing structures allows companies to plan energy consumption effectively and optimize costs [8]. Developing strategies to mitigate the impact of load shedding is crucial for ensuring uninterrupted production. Furthermore, identifying peak demand periods and implementing load management strategies can help industries optimize electricity usage and avoid excessive demand charges. Compliance with energy codes and standards is another important aspect of managing electricity demand. Adhering to regulations related to energy efficiency, building codes, and

electrical systems ensures that textile industries operate in an environmentally responsible and sustainable manner. By following energy codes and standards, companies can improve their energy performance, reduce waste, and contribute to a greener future [13,14]. In conclusion, the textile industry's electricity demand is driven by its energy-intensive processes and reliance on machinery [15]. Through a combination of measures such as energy efficiency, renewable energy integration, and smart energy management, the industry can address its electricity demand and reduce its environmental impact. Implementing energy management strategies, conducting energy audits, optimizing power factor, and utilizing energy storage systems are essential steps in optimizing electricity consumption. Energy conservation practices, smart grid integration, and the use of variable speed drives contribute to further energy savings [14]. Considering factors such as energy tariffs, load shedding, and compliance with energy codes and standards are crucial for effective electricity management. By adopting these measures, the textile industry can achieve sustainable and efficient electricity usage while maintaining productivity and competitiveness in the global market [8, 13, 15]. In addition to the aforementioned measures, electro-kinetic energy plays a crucial role in the textile industry's electricity management. Electro-kinetic energy refers to the conversion of mechanical energy into electrical energy, which can be utilized to meet the industry's electricity demand. Textile machinery, such as spinning machines, looms, and knitting machines, often generate mechanical energy during their operation. This mechanical energy can be harnessed and converted into electrical energy through the use of regenerative braking systems and energy recovery devices. By capturing and utilizing this electro-kinetic energy, textile industries can significantly reduce their electricity consumption and overall energy costs. Regenerative braking systems, for example, allow the recovery of kinetic energy that would otherwise be dissipated as heat during the deceleration or stopping of machinery. This recovered energy can be fed back into the electrical grid or stored for later use, thereby reducing the amount of electricity required from external sources. Similarly, energy recovery devices, such as flywheel energy storage systems, can capture and store excess mechanical energy during peak production periods. This stored energy can then be released during high electricity demand periods, providing a supplemental power source and reducing reliance on conventional electrical supply. The integration of electro-kinetic energy technologies offers significant advantages for the textile industry. Not only does it contribute to overall energy

savings, but it also enhances the energy efficiency and sustainability of textile manufacturing processes. By effectively capturing and utilizing electro-kinetic energy, textile industries can reduce their environmental impact, lower electricity costs, and improve their overall energy performance. In conclusion, the textile industry can benefit greatly from the incorporation of electro-kinetic energy technologies in its electricity management strategies. By harnessing the mechanical energy generated by textile machinery and converting it into electrical energy, textile industries can reduce their reliance on external electricity sources and achieve greater energy efficiency. The integration of regenerative braking systems, energy recovery devices, and other electro-kinetic energy technologies can lead to significant energy savings, cost reductions, and environmental benefits. Combined with other measures such as energy efficiency, renewable energy integration, and smart energy management, electro-kinetic energy plays a vital role in optimizing electricity consumption in the textile industry and ensuring its long-term sustainability. The study flow encompasses a thorough background analysis, a summary of relevant literature, the development of a theoretical framework, and the implementation of experimental sources to further investigate and improve the low cost electro-kinetic energy extraction from weaving power looms by using Uni/Bi-Directional Weaving actions.

2. BACKGROUND ANALYSIS

2.1. Existing Industrial Energy Harvesting Methodologies and Its Problems

India and China hold prominent positions in textile cultivation, their cotton, woolen, and silk fabrics being highly sought after by numerous countries due to their superior quality and cost-effectiveness [2, 9]. The textile industry in India, in particular, stands as the second-largest employer, second only to agriculture. It encompasses a vast array of both manual and non-manual processes including weaving, spinning, knitting, wet processing, and garment manufacturing. These processes, illustrated in Figure 1 (Textile Industries Sub Manual and Non-Manual Process), necessitate specific electric drives such as permanent magnet synchronous motors, squirrel cage induction motors, and single-phase induction motors, each of which can operate at either variable or fixed speeds based on their functionality subclass. The specifics of speed control for power drives are explored in depth in Paper 40, which investigates advanced controllers utilizing power electronics interfaces. The study focuses on industrial adjustable-speed

drives and their control strategies, utilizing voltage source inverters with space vector pulse width modulation while incorporating a fuzzy-PI controller. Furthermore, Paper 48 highlights critical factors influencing the business growth of the power loom industry, as visualized in Figure 2 (Factors Affecting Power Loom Industry Business Growth). Among these, frequent power shortages are a significant concern faced by power loom industries. Consequently, a substantial portion (50–70%) of medium and large-scale industries resort to diesel power generators to ensure uninterrupted textile production, subsequently leading to increased power loom maintenance expenses. Numerous power loom weavers express apprehensions regarding the elevated power costs in comparison to other regions such as Andhra Pradesh and Maharashtra. To address this, the Tamil Nadu Electricity Board has allocated 750 units of free electricity to power loom industries

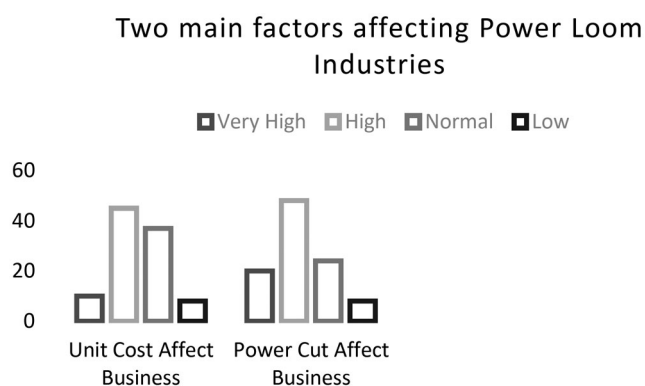


FIGURE 2. Factors are affecting power loom industry business growth.

[9]. Nevertheless, this allocation often falls short for the weaving process, and as a result, the productivity of various industries indirectly hinges on non-renewable power sources. In view of the global impetus on renewable energy sources to achieve greenhouse gas (GHG)-free and sustainable industrial power generation, the primary objective of this project is to advance the electrokinetic energy extraction model from power loom applications [11, 16]. The textile, food, and agricultural cultivation sectors exhibit significant electricity demands, making them heavily reliant on dependable energy sources. To fulfill these requirements, industrial energy harvesting methods are commonly employed, drawing from renewable, semi-renewable power sources, as well as external power grids. Table 1 (Industrial Energy Harvesting Methodologies), referencing sources [4, 17], and [18,19] presents an overview of various technologies utilized for continuous electricity extraction.

The industrial energy harvesting methodologies predominantly rely on solar photovoltaics and micro wind turbines as primary sources [20–25]. However, these strategies are subject to natural factors and power conversion limitations. Solar energy generation is contingent upon factors such as solar radiation quantity and weather conditions [22, 24, 26,27], while wind energy extraction is reliant on wind density [9, 13]. Both methods are primarily applicable to outdoor energy harvesting processes. Moreover, the manufacturing of solar cells involves the use of organic and inorganic materials, resulting in indirect greenhouse gas emissions [28–30]. In contrast, micro wind turbines offer greenhouse gas-free power generation, but their output is heavily influenced by wind density, leading to intermittent

S.No	Principles	Sources	Harvesting applicable	Geo-graphical/weather dependable
1	Photo-voltaic	Solar-rays	Outdoor	Fully depended
2	Electro-kinetic energy	Micro wind turbine	Outdoor	Fully depended
3	Peltier/See beck effect	Thermo-electric cells	Indoor and Outdoor	Partially depended
4	Kramer/Scribus	Slip ring induction motor	Indoor	Fully independent
5	Electro-magnetic induction	Fly wheel & linear generation	Indoor and Outdoor	Fully independent
6	Piezo electric effect	Piezo cells	Indoor and Outdoor	Fully independent
7	Combined cool and heat power	Co-generation & tri generation	Hybrid	Fully depended
8	Captive power units	Diesel/natural gas	Hybrid	Fully depended
9	Hybrid power sources	Solar, fuel cell, micro wind turbine	Hybrid	Fully depended

TABLE 1. Industrial energy harvesting methodologies.

power generation. Given these considerations, researchers and industrial engineers are actively exploring renewable power sources and conducting studies in these areas. They investigate techniques such as AI and machine learning-

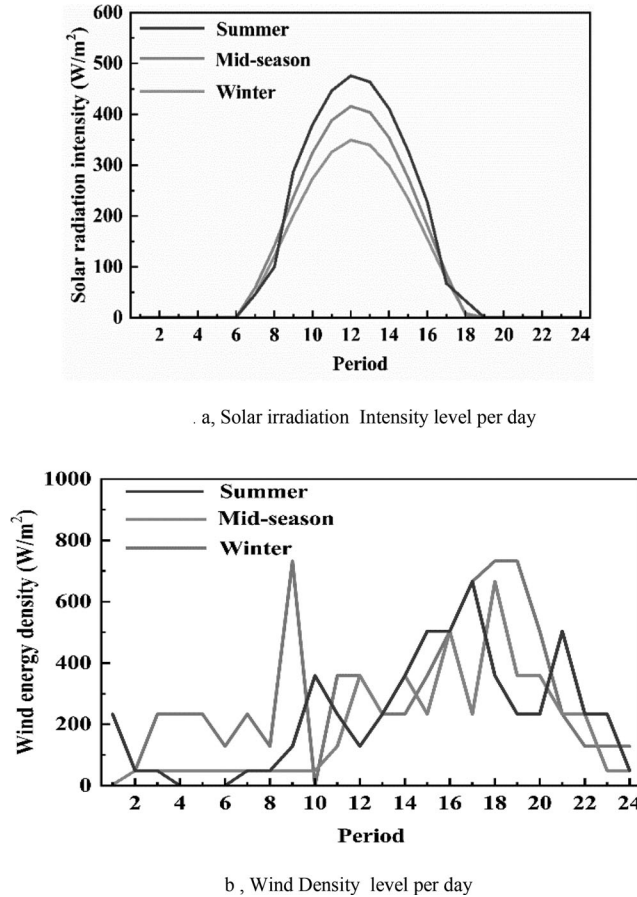


FIGURE 3. Per day data of solar intensity and wind density.

based solar and wind power forecasting, advanced DC-DC power conversion, battery energy storage, and power factor correction to ensure continuous power supply to loads [22, 25, 31,32]. Additionally, force-based renewable power extraction is being investigated as a stable alternative to solar and wind energy sources [2]. This project specifically focuses on force-related renewable power extraction, acknowledging its stability compared to solar and wind sources, as referenced in sources [17,18, 33], and [34]. Figure 3 (a. per day data of solar intensity and b. wind density), referenced from source [33], provides a graphical representation of the daily variations in solar intensity and wind density.

Numerous research papers have concentrated on the advancement of force-related kinetic renewable power harvesting technologies. These technologies have found applications in wireless networks, biomedical devices, and Pavegen paths. They utilize various mechanisms such as mechanical vibration rectifiers, electromagnetic induction, and thermoelectric generators. The motivation behind these advancements stems from the fact that many industrial processes result in the dissipation of electrical energy into non-usable and non-storable forms, such as thermal energy, mechanical energy, light, and sound energy.

In response to this energy degradation, indoor industrial energy optimization technologies have been proposed. These technologies aim to harness the degenerated energy within industrial environments and convert it into regenerative energy. This can be achieved by utilizing the kinetic and thermal energy utilities present in industrial indoor settings. Papers 5 and 34 provide valuable insights into industrial energy consumption and offer recommendations for energy optimization strategies. Table 2 (thermal and kinetic

Degenerating energy form	Textile industries sub-non-manual process	Usable energy forming methodologies
Electrical energy to thermal energy	Scouring process Shrinking & bleaching process Dyeing & washing process Heat setting process Printing process Color setting process Washing process Hydro extraction process Pressing process Packing/dispatch	Steam based co-generation, cool based co-generation, energy efficient pumps, heat recovery from hot drained water, pressurized power pumping unit and steam traps
Electrical energy to mechanical energy	Weaving Sewing	Nil

TABLE 2. Thermal and kinetic energy degeneration from textile industries sub non-manual process.

energy degeneration from textile industries sub-non-manual processes), as presented in sources [4, 35], provides a comprehensive overview of the utilities associated with the degeneration of thermal and kinetic energy in textile industry sub-non-manual processes. This table serves as a reference point for understanding the potential energy sources available for harvesting and optimization in industrial settings.

Table 2 (Thermal and Kinetic energy degeneration from textile industries sub non-manual process) does not include specific information about the conversion of kinetic energy to usable energy in the weaving and sewing sub-manual processes. However, Paper 46 offers more detailed insights into energy loss statistics within the textile industry, with a particular focus on the U.S. textile sector. The motor-driven systems are found to be responsible for the highest share of energy loss, accounting for approximately 36%. This energy loss occurs due to the inefficient conversion of electrical energy into kinetic energy, resulting in undesired rotation and movement of steel bodies. Figure 4 (Various Energy loss statistics of US Textile cultivation) illustrates the distribution of energy loss in various factors within the U.S. textile cultivation. Furthermore, Paper 46 provides an overview of electricity consumption across different sub-non-manual processes in the textile industry, which may vary depending on the industry’s scale. According to Figure 5 (4 Energy Consumption of Textile industries entities), spinning processes have the highest electricity consumption share at around 41%, followed by weaving preparation and weaving processes at 18%. Other processes, such as wet processing, heavily rely on thermal energy consumption, representing 35% of the overall energy consumption. Notably, the weaving entities consume a significant portion, ranging from 50% to 60%, of

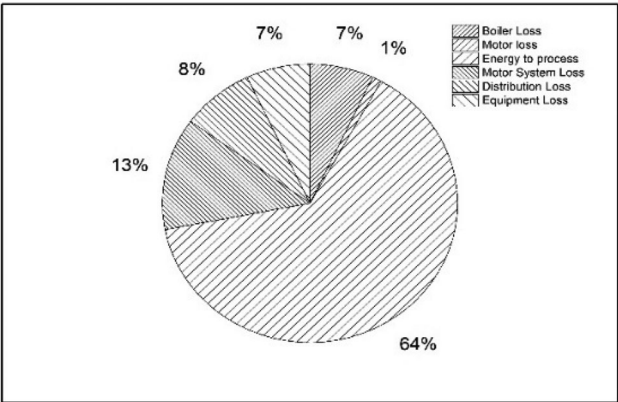


FIGURE 4. Various energy loss statistics of US textile cultivation.

the electrical energy used in the looming industries. Improving energy efficiency in weaving, therefore, presents a crucial opportunity for enhancing the overall energy efficiency of textile cultivation. Given the significance of the weaving process and its contribution to energy consumption, our research specifically focuses on sub-non-manual weaving processes. While different types of weaving machines exist, they all incorporate various mechanisms that involve the processing of kinetic energy. By exploring methods to optimize the conversion and utilization of kinetic energy within the weaving process, we aim to contribute to the broader goal of enhancing energy efficiency in the textile industry [35].

2.2. Analysis of Alternative Energy Sources from Industrial Energy Harvesting Units

The Literature 5 and 34 papers propose three kinetic energy harvesting mechanisms, as depicted in Figures 6 (Piezoelectric effects), Figure 7 (Linear power generation due to vertical kinetic energy) and Figure 8 (Non-linear Power Generation due to Rotational Kinetic energy). However, this project specifically focuses on the utilization of piezoelectric methods to extract kinetic energy from weaving applications. Piezoelectric effects occur when mechanical strain is applied to piezoelectric materials, resulting in the generation of an electric field within the material. This phenomenon is illustrated in Figure 6(a) Strain Applied to Piezo Material, Figure 6(b) Electronegativity of Piezo-cell, Figure 6(c) Electron Flow Model of Piezo-Cell. To assess the efficiency of mechanical-to-electrical energy conversion in the piezoelectric harvester, we can consider the mechanical input and electrical

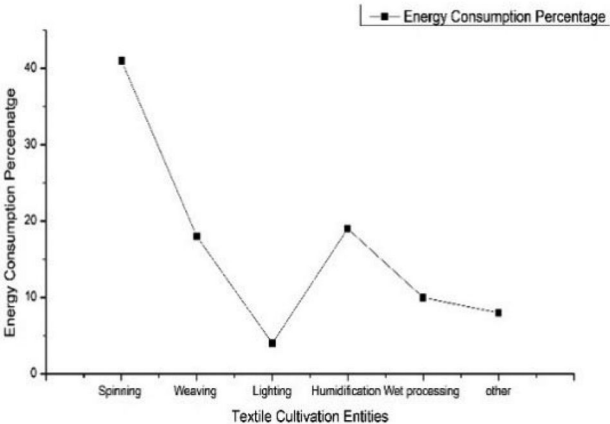


FIGURE 5. Energy consumption of textile industries entities.

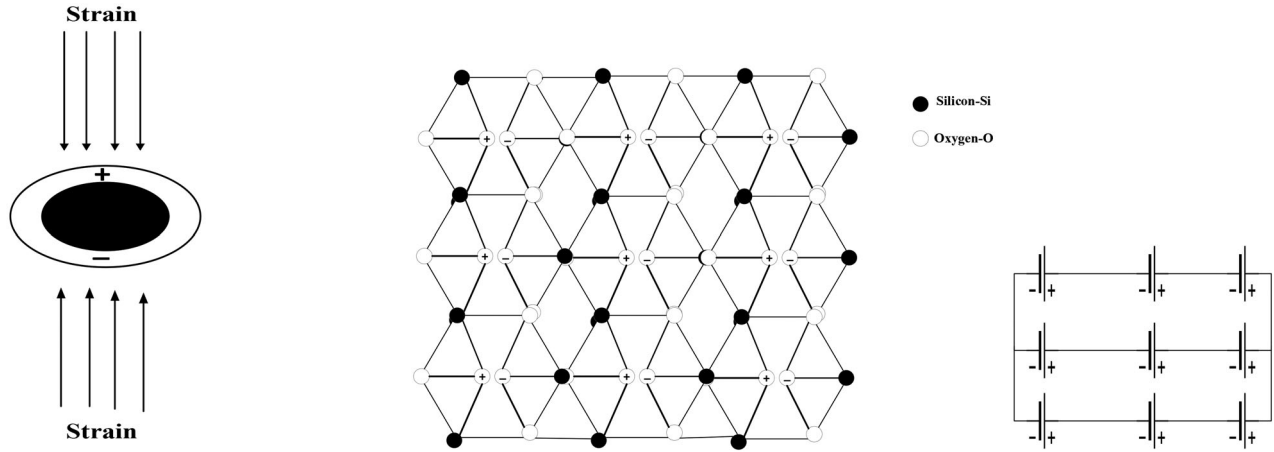


FIGURE 6. (a) Strain applied to piezo material. (b) Electronegativity of piezo-cell. (c) Electron flow model of piezo-cell.

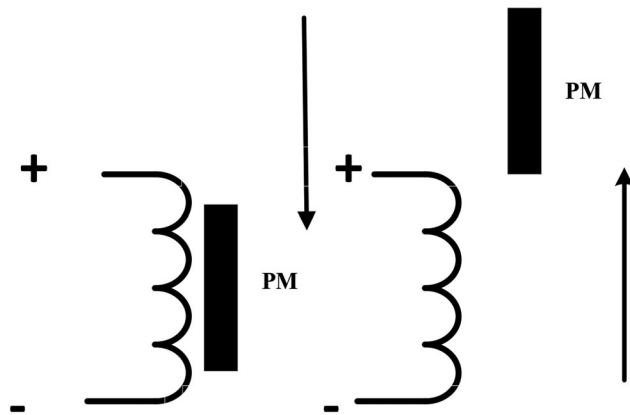


FIGURE 7. Linear power generation due to vertical kinetic energy.

output. The efficiency can be calculated by comparing the amount of electrical energy generated to the mechanical energy input. This calculation allows us to evaluate the performance and effectiveness of the piezoelectric harvester in converting mechanical strain from the weaving process into usable electrical energy. The specific equations for this calculation are as follows:

$$E\% = \frac{P_{out}}{P_{in}} \times 100 \quad (1)$$

P_{out} -is electrical output

$$P_{out} = V_p \cdot I_p \quad (2)$$

P_{in} -is Mechanical input

$$P_{out} = F \cdot v \quad (3)$$

where V_p -total voltage generated from piezo-electric output terminal; I_p -output current due to piezo electric effect; F -external mechanical force; v -speed of moving object.

Piezoelectric materials used for electro-kinetic energy harvesting include various subtypes, such as Lead Zirconate Titanate (LZT), Lead Magnesium Niobate, Lead Titanate, and Polyvinylidene Fluoride (PVDF). LZT and PVDF are widely utilized in aerospace and automotive applications. Additionally, there are other piezoelectric materials specifically designed for electro-kinetic energy harvesting, including single-crystal piezoelectric materials, high-temperature piezoelectric materials, piezoelectric foams, and other piezoelectric-based methods. The effectiveness of piezoelectric energy harvesting methods relies on two crucial factors: the selection of the appropriate piezoelectric material, such as LZT and PVDF, and the configuration of the piezoelectric energy harvesting circuit.

[Table 3](#) (Piezoelectric Energy Harvester Configuration

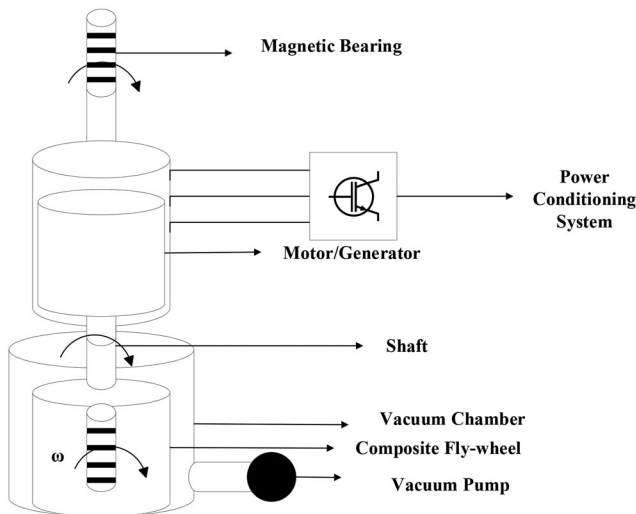


FIGURE 8. Non-linear power generation due to rotational kinetic energy.

Configuration details	Layers	Energy level
Cantilever beam (unimorph)	Single layer piezo	Low
Cantilever beam (bimorph)	Two layer piezo	Medium
Circular diaphragm	Circular piezo layer	Medium
Cymbal type	Single layer width more	High
Stacked type	Multi-piezo layer	High

TABLE 3. Piezo-electric energy harvester configuration types.

PEH model	Electric Energy output level	Expensive level
Drum harvester	~2.463 mW	Low
BATiO3	~7mW	Low
Waynergy	10W	High
Sustainable Energy floor	Up to 30 W	High
Pavegen	~5 W	Very high

TABLE 4. High amount of piezo-electric energy harvesting model details.

Types) provides an overview of the available piezoelectric energy harvester circuits, as depicted in the literature references [36] and [7]. These circuits offer different configurations and characteristics to optimize the conversion of mechanical strain into electrical energy, allowing for efficient energy harvesting from weaving applications.

The table referenced as 3 (Piezo-electric Energy Harvester Configuration Types) provides detailed information on various configurations of piezoelectric energy harvesters, including energy levels. It highlights the technical dependencies involved in piezoelectric energy harvesting, such as the connection of piezoelectric arrays and the characteristics of kinetic utilities. In weaving applications, different types of kinetic utilities are utilized, including horizontal and vertical weaving moment mechanisms and the design of zig-zag wooden rectangular patterns. However, for this project, the focus is specifically on the analysis of electrokinetic energy extraction based on the kinetic utilities of designing printing zig-zag wooden rectangular patterns and horizontal weaving read pattern. The aim is to utilize piezoelectric plates from a power loom weaving machine for energy harvesting. Furthermore, paper 25 provides additional literature on various piezoelectric-related topics. It presents a wide range of piezoelectric energy harvester models and provides information on their commercial availability. Table 4 (High amount of Piezo-electric Energy Harvesting Model Details) presents comprehensive details about these models,

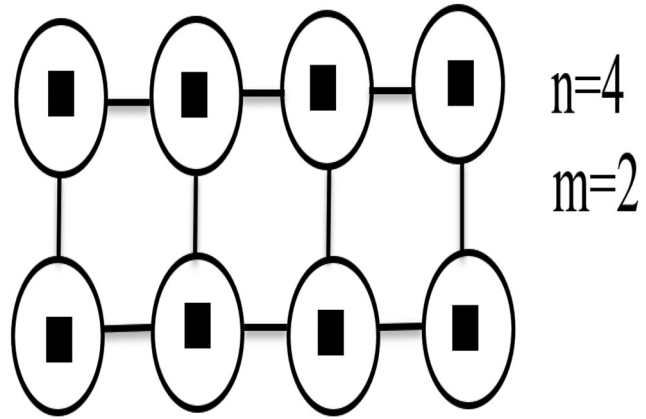


FIGURE 9. Series-parallel piezo cells connection.

including their specifications and availability in the market. This literature can serve as a valuable resource for understanding the different options and possibilities in piezoelectric energy harvesting.

The cost of piezoelectric energy harvesters tends to increase when higher amounts of electro-kinetic energy are required. To address this, most piezoelectric energy harvesters are designed using a series-parallel piezo array model. This configuration ensures that the combined output of the piezo array matches the desired energy level. In a series-connected piezo cell configuration, the voltage output is good, but the current output is poor. On the other hand, parallel-connected piezo cells provide good current output but may not deliver optimal voltage. To overcome these limitations, a hybrid connection of series-parallel piezo cells is utilized. By connecting the cells in a series-parallel configuration, both the output voltage and current can be improved. Figure 9 (Series-Parallel Piezo Cell Connection) [37] illustrates the series-parallel connection of piezo cells, depicting how they are interconnected. This configuration enables better optimization of both voltage and current outputs. Paper 20 provides comprehensive details on the output current and voltage levels of series-parallel piezoelectric plates, as shown in Figure 10 (Series-Parallel Piezo Plates V-I Characteristics) [37]. This information is valuable for understanding the performance characteristics of series-parallel piezo plates and their suitability for electro-kinetic energy harvesting applications.

2.3. Analysis of Piezo-Electric Harvesters with Power electronics Interfaces

To optimize the performance of piezoelectric harvesters, it is necessary to integrate power electronics interfaces, as

the output of the piezo-array is typically in the form of alternating current (AC). AC-DC power conversion is required to make the harvested energy usable. This conversion can be achieved through the use of a bridge rectifier or a resonance rectifier, depending on the specific requirements of the application. If the generated energy needs to be stored for later use, the fixed DC power output from the rectifier must be converted to variable DC power. This can be accomplished using various chopper circuits that regulate the voltage or current levels as needed. In the context of this project, a secondary objective is to design a feasible DC-DC converter specifically tailored for a piezoelectric energy harvester. The literature papers [38–40] discuss power electronics interfaces and provide insights into the design and implementation of these converters. Paper 18 further elaborates on the circuit elements of a vibration-based piezoelectric energy harvester, as illustrated in Figure 11 (Vibration-based Piezoelectric Energy Harvester

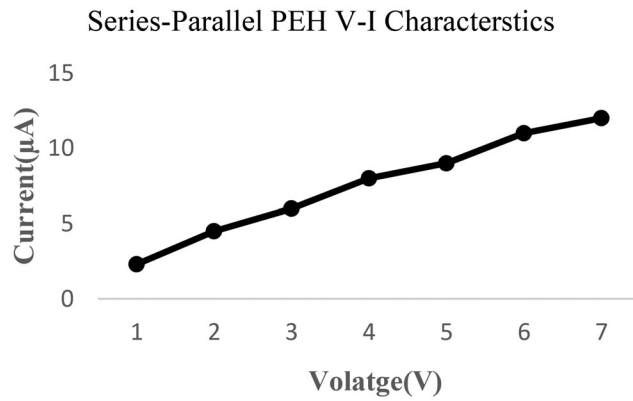


FIGURE 10. Series-parallel piezo plates V-I characteristics.

Circuit Model). This circuit model serves as a valuable reference for understanding the components and connections involved in a vibration-based piezoelectric energy harvesting system.

The output voltage of a piezoelectric energy harvester is typically low due to the impedance mismatch between the piezoelectric material and the external resistive load. To address this issue, various power electronics interfaces have been explored, as discussed in Papers 1, 2, and 3. Table 5 (Summary of PEH Power Electronics Interface) provides a summary of these power electronics interfaces, outlining their characteristics and advantages. Among the power electronics interfaces, the boost converter model requires an intelligent controller to optimize the performance of the piezoelectric harvester. On the other hand, the flyback converter operates in a closed-loop system and generally offers better efficiency compared to the boost converter. Figure 12 (Fly-Back Converter based Piezo-electric energy harvester) illustrates the operation of a flyback converter. In the pursuit of improved efficiency, series and parallel synchronized switch harvesters on inductors have been investigated, as highlighted in Papers 4, 38, and 23. Paper 38 specifically delves into the parallel SSHI-based piezoelectric energy harvester, depicted in Figure 13 (Parallel SSHI based Piezo electric energy harvester). Both series and parallel synchronized switch harvesters exhibit similar efficiency levels. The model presented in Figure 13 (Parallel SSHI based Piezo electric energy harvester) generates 5 VDC with an input of 0.7 VAC. However, it should be noted that the parallel SSHI-based piezoelectric energy harvester may not be suitable for variable loads. In the context of renewable power sources, advanced DC-DC

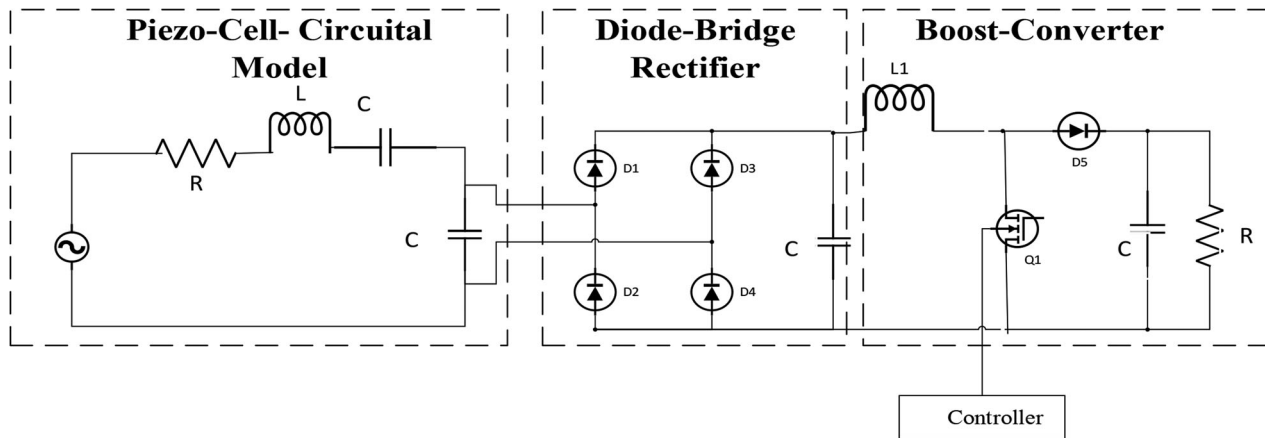


FIGURE 11. Vibration based piezo-electric energy harvester circuit model.

Power electronics interface (Second level power conversion)	Controllability	Feedback stability	Efficiency
Boost converter	Variable	Good	Medium
Two stage boost converter	Variable	Good	Low
Fly-back converter	Variable	Good	Medium
Series synchronized switch harvesting on inductor	Fixed	Not-present	High
Parallel synchronized switch harvesting on inductor	Fixed	Not-present	High

TABLE 5. Summary of PEH power electronics interface.

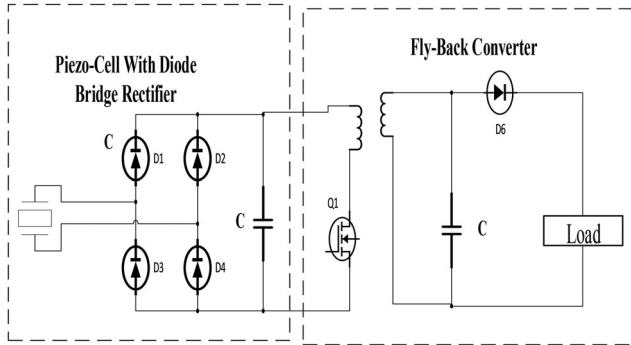


FIGURE 12. Fly-back converter based piezo-electric energy harvester.

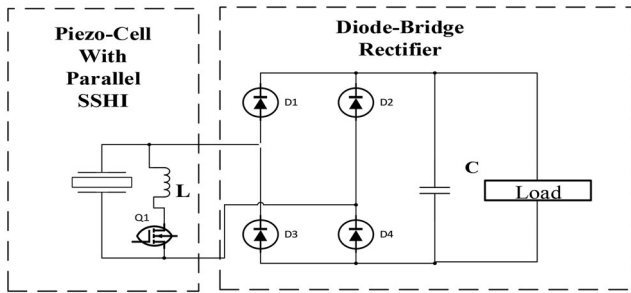


FIGURE 13. Parallel SSHI-based piezo electric energy harvester.

converters play a crucial role [41]. Paper 9 provided comprehensive analysis of various Converter topology with suitable energy sources [41]. The overall literature suggests the utilization of the super lift Luo converter and Zeta converter to increase the output voltage while reducing ripple content and improving feedback stability [38–40, 42]. Therefore, for this project, a second-level power conversion is implemented using a super lift Luo converter, which offers enhanced voltage boosting capabilities and improved stability. This converter facilitates the efficient utilization of the harvested energy from the piezoelectric energy harvester.

3. SUMMARY OF SURVEY

The Summary of Background Analysis given 6 (Summary of Background Analysis Narrow Down Details)

As per Table 6, observation system configuration details are given in Figure 14 (Theoretical frame work flow chart).

In this subsection, the measurement and calculation of kinetic utilities from power loom applications will be conducted to identify the various sources of kinetic energy in different types of weaving machines. This analysis will lead to the final design of kinetic utilities specific to the weaving process. Understanding the terminology associated with weaving machines will aid in identifying all the peripherals that generate kinetic energy during the weaving process. The configuration of piezo plates will be thoroughly discussed, considering the selection of suitable piezo plates and their appropriate connection. This step is crucial for optimizing the performance of the piezoelectric energy harvester. The power electronics interface section will provide detailed information about the harvester circuit, covering both the first-level and second-level power conversion. The first-level power conversion involves the AC-DC conversion using techniques such as bridge rectifiers or resonance rectifiers. The second-level power conversion focuses on utilizing advanced DC-DC converters like the super lift Luo converter to further enhance the output voltage and stability of the system. Furthermore, the energy estimation derived from the designed energy harvester will be presented, providing insights into the efficiency and potential energy generation of the system. Suggestions for further improvement and refinement of the project will also be discussed, aiming to optimize the overall performance and energy harvesting capabilities of the designed system. By addressing these aspects, a comprehensive understanding of the kinetic energy harvesting process in power loom applications will be achieved, leading to the development of an efficient and effective energy harvesting system for the weaving industry.

Ref Paper	Details	Summary Details
[1–6, 8, 14–16, 43,44]	Factors Affecting Textile Cultivation	Investigates the multifaceted factors influencing textile cultivation, delving into the impact of electric power demand, cost per unit, and the role of electric drives in optimizing production processes.
[35, 45]	Non-Manual Processes and Electric Drives in Textile Industry	Explores the integration of electric drives in non-manual textile processes, elaborating on specific speed drive types employed and control strategies applied for improved efficiency.
[45]	Industrial Electric Drives Demand and Control	Provides an in-depth analysis of the demand for industrial electric drives, elucidating their characteristics and the strategic application of drive speed control to enhance overall productivity within the industrial production chain.
[9, 11, 13, 17–21, 23–31, 33,34, 46,47]	Industrial Energy Harvesting Approaches	Explores a diverse array of indoor and outdoor energy generation methods suitable for industrial applications, focusing on sustainable energy harvesting for improved efficiency.
[4, 35]	Energy Loss in Textile Industry and Recovery	Investigates the magnitude of thermal and kinetic energy losses in the textile sector, showcasing strategies for recovering and converting these losses into usable electrical energy, ensuring enhanced efficiency.
[10, 17,18, 36]	Kinetic Energy Harvesting Techniques	Examines various methods for harvesting kinetic energy, such as piezo plates, fly-wheels, and linear generation, discussing their potential for transforming mechanical motion into valuable electrical energy.
[7, 12, 37, 48]	Piezoelectric Materials and Configuration Analysis	Explores the nature of piezoelectric materials, delving into different configuration types, conducting an output efficiency analysis, and tracing the evolutionary trajectory of piezoelectric technologies.
[22, 32,33, 38–42, 49]	Power Electronics Interface Assessment	Provides a comprehensive overview of power electronics interfaces, analyzing AC-DC and DC-DC power conversion strategies, and their pivotal role in facilitating efficient energy conversion across diverse contexts.

TABLE 6. Summary of background analysis narrow down details.

4. THEORETICAL FRAME WORK

4.1. Measurement and calculation of Kinetic Utilities from power Looms

According to the observation in Figure 1 (Textile Industries Manual and Non-Manual Processes), weaving holds a significant position in textile cultivation. Weaving can be carried out using handlooms or power looms. The primary objective of weaving is to create the structural framework of clothes through vertical and horizontal cross-

sectional threading. Typically, the weaving process involves the use of a squirrel cage induction motor for constant speed operation. Figure 15 (Architecture of power loom energy transforming model) illustrates how power loom applications extract energy from an external power grid, input mechanical energy produced by electric drives, and transform the mechanical energy through lengthy open-wheel pipelines. The weaving subunit is integrated in the middle of this pipeline due to its mechanical motion. This integrated subunit is responsible for carrying

Theoretical Frame work :

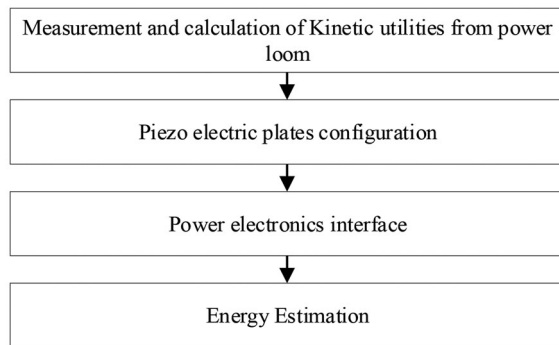


FIGURE 14. Theoretical frame work flow chart.

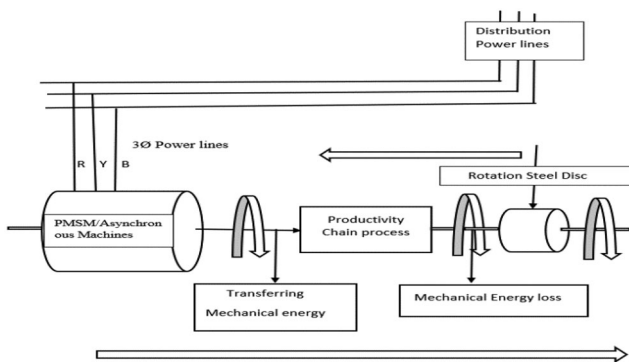


FIGURE 15. Architecture of power loom energy transforming model.

out the weaving process. The weaving subunit consists of various components, including the warp beam, cloth roll, filling carriers, filling yarn, warp yarn, harness, and a heated frame, which are all essential for design printing. The structure of the weaving machine may vary depending on the cloth design, such as jacquard, bullet loom, water jet looms, etc. Figure 16 (Typical power diagram of Weaving Process) illustrates the basic architecture of the weaving process, the weaving carrier filing process, and the bi-directional yarn filing with the horizontal movement of the reed. This horizontal movement of the reed contributes to a certain amount of kinetic energy. Similarly, the design printing head frame also undergoes an up and down movement, resulting in the generation of vertical moment kinetic energy. Therefore, the weaving process generates both vertical and horizontal kinetic utilities. The vertical kinetic energy produced by the head frame varies among different looms. In this project, the auto loom head frame and the Horizontal Open-end Reed will be considered for their kinetic utilities. Typically, the head frame of the

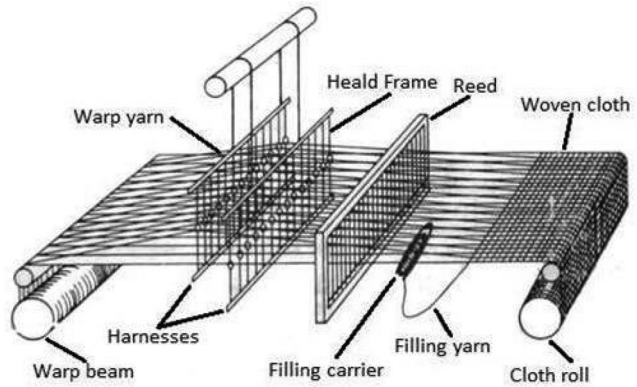


FIGURE 16. Typical power diagram of weaving process.

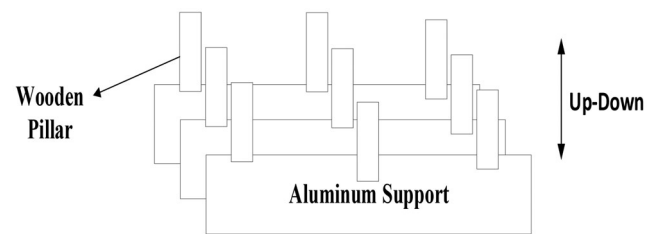


FIGURE 17. Head frame model.

loom machine is a combination of wooden pillars and a supportive aluminum body. The wooden pillars are the source of kinetic energy in this context, as they exert a significant force. Each frame usually contains three or four wooden pillars. The combination of these three head frames is depicted in Figure 17 (Head frame structure).

The wooden pillars of the head frame move up and down according to the printed design. There are two types of head frames: closed-end and open-end. The closed-end head frame is connected to a design printing unit, such as a mechanical or electronic jacquard, and it does not generate kinetic energy from the weaving process. The up-down movement of the closed-end head frame depends on the instructions from the jacquard machine, as depicted in Figure 18 (Closed end Head Frame Arrow Notation), Figure 19 (Open end Head Frame Arrow Notation). On the other hand, the open-end head frame acts as a unidirectional kinetic energy producer. Since there are no instructions coming from the closing end, the open-end head frame integrates the weaving instructions within the loom bottom unit. This allows it to continuously generate kinetic energy through the up and down movement of the top unit. A single aluminum frame typically contains three wooden pillars, and each pillar requires a separate piezo harvester unit. Therefore, approximately nine piezo harvester units

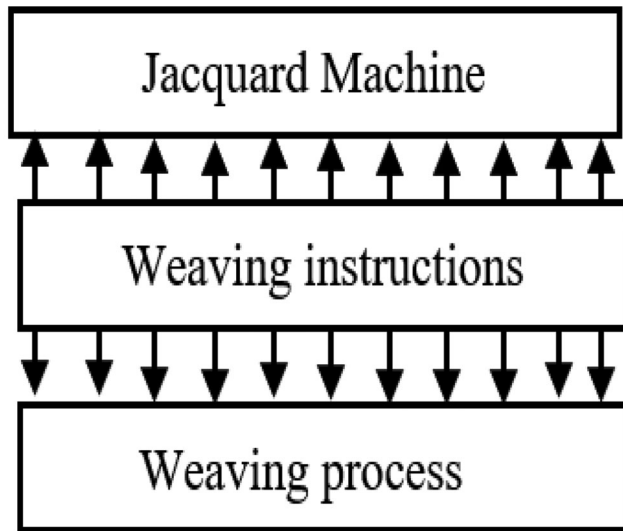


FIGURE 18. Closed end head frame arrow notation.

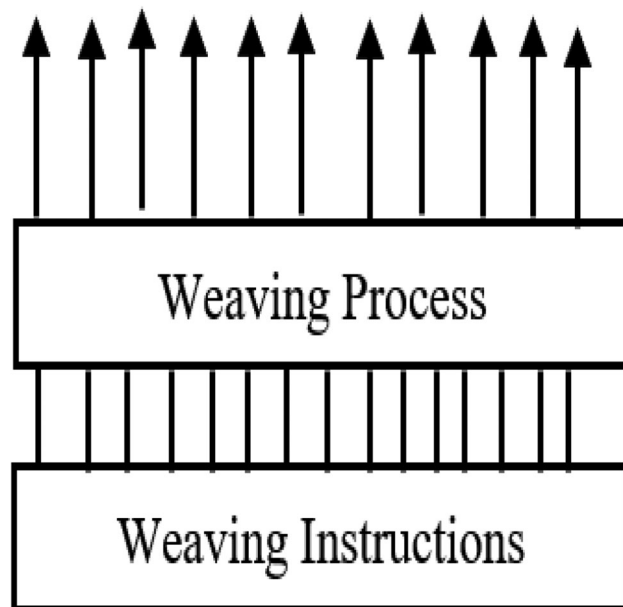


FIGURE 19. Open end head frame arrow notation.

are required for a single open-end head frame. The area of each wooden pillar is calculated as 40 square units, as shown in Figure 20 (Area Calculation of Wooden Pillar). The pillars are usually made of materials like red wood or play wood, and their weight is less than or equal to 1 kg, depending on the density of the wood. The velocity of the pillar is 0.3 m/s, and the force exerted is 0.3 N. In the case of the closed head frame with jacquard machines, the yarn filing read moves horizontally. The actual design of the read unit can be seen in Figure 21 (Horizontal Yarn Read

Model). The area of the open-end read is calculated as shown in Figure 22 (Area Calculation of Open-end Read). The total weight of the open-end read is approximately 50 kg, and the velocity and force of the horizontal yarn read are both 0.3 m/s and 0.3 N, respectively. Based on the kinetic energy produced, suitable piezoelectric plates will be designed for energy harvesting purposes.

4.2. Piezo-Electric Plates Configuration

To design nine piezo plates for the nine kinetic energy producers, each piezo plate will consist of a 4×2 configuration of piezo cells. In this configuration, a single row contains four piezo cells, and there are two rows in total. The piezo cells are arranged in close proximity to each other and connected in a series-parallel configuration. The electrical power output of the piezo cells depends on the amount of pressure applied and the quality of the piezo cells. In the case of foot path-based piezoelectric generation, it was reported that a 75 kg object with a single piezo tile (4×2 piezo array) can produce 40 V of voltage, as observed in Figure 10 (Series-Parallel V-I Characteristics). Based on this observation, the calculated current is approximately 68.57×10^{-6} A, and the total power of the piezo tiles is approximately 2.742×10^{-3} [22]. There are two ways to integrate the piezo array with the kinetic energy producers. One approach is to integrate the piezo plates with the T-joint shape of the wooden pillars of the kinetic energy producers. The other approach is to use a double-layer integration method. The designs for these piezo harvester configurations can be seen in Figure 23 (Piezo-Plates Integration with Movable Wooden Pillar) and Figure 24 (Piezo-Plates Integration with Horizontal Yarn Open End Read), respectively.

4.3. Power electronics Interface

The power electronics interface plays a crucial role in connecting the piezo harvester unit to the load or energy storage system. Since the piezo harvester unit generates AC voltage, and the project aims to integrate it with a DC microgrid, a conversion from AC to uncontrolled DC voltage is required. This uncontrolled DC voltage is then further processed through second-level power conversion, where it undergoes DC-DC conversion with a boosting mode using an advanced DC-DC converter. Figure 25 (Open Head frame with Piezo harvester (4×2)) and Figure 26 (Open-end Read with Piezo harvester (2×10)) provides a description of the power electronics interface with the piezoelectric harvester, illustrating the conversion

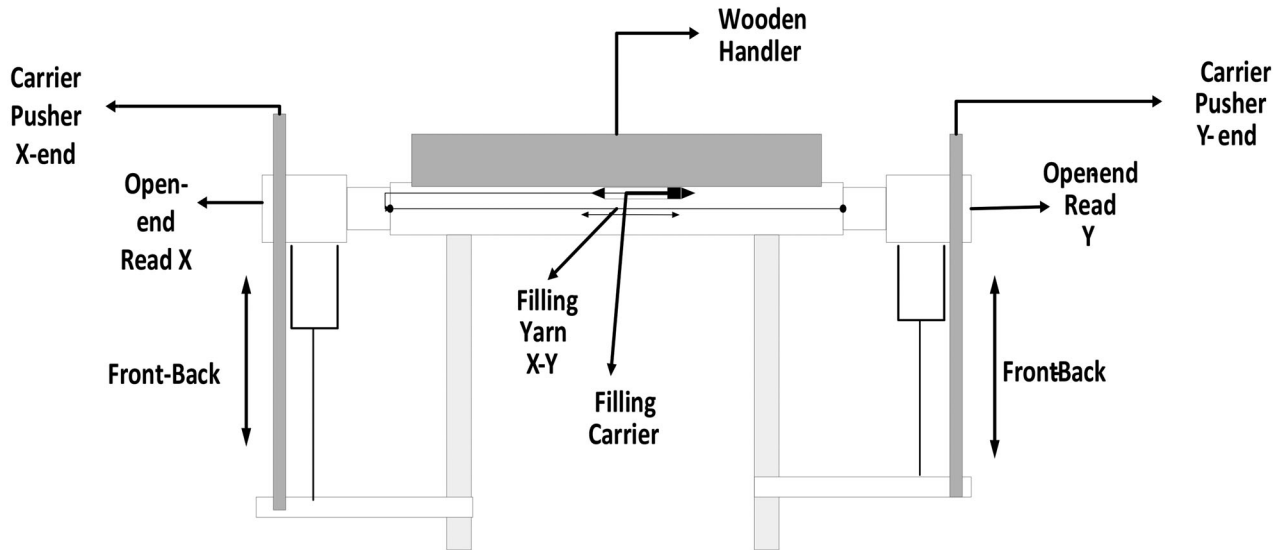


FIGURE 20. Horizontal yarn read model.

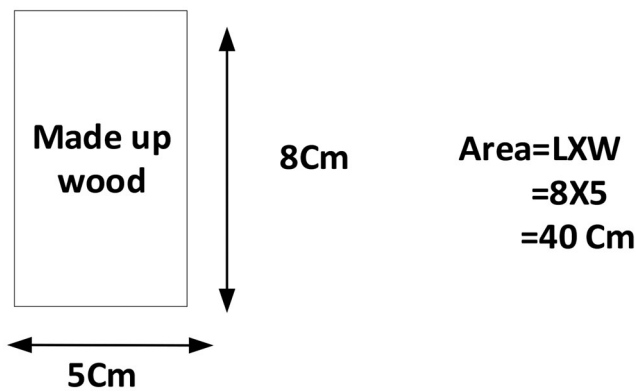


FIGURE 21. Area calculation of wooden pillar.

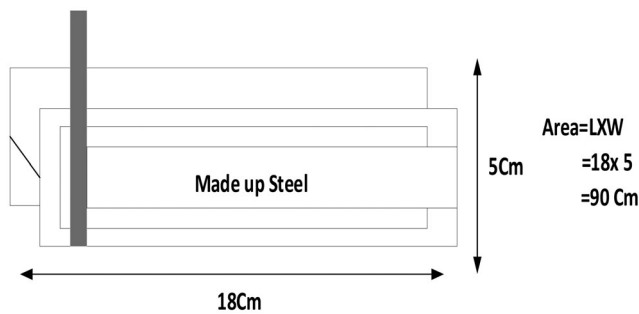


FIGURE 22. Area calculation of open end-read.

process and the components involved in the interface. This interface ensures that the AC voltage generated by the piezo harvester is converted and regulated to a suitable DC voltage for utilization within the DC microgrid system.

As per Figure 25 (Open Head frame with Piezo harvester (4×2)) and 26 (Open-end Read with Piezo

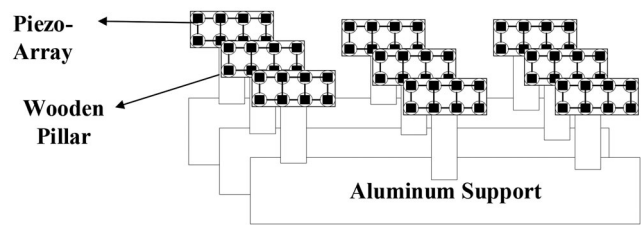


FIGURE 23. Piezo-plates integration with movable wooden pillar.

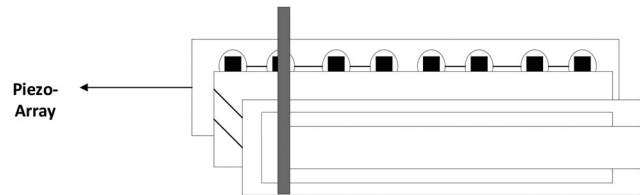


FIGURE 24. Piezo-plates integration with horizontal yarn open end read.

harvester (2×10)), the output of the piezo harvester is connected to a capacitor unit. This is because the kinetic energy production from the open-end read and movable wooden pillar follows a push-pull-push-pull pattern, resulting in a single instance of kinetic energy being converted to electrical energy. Each piezo cell can produce a maximum of 3 V AC and a minimum of 0.7 V AC, depending on factors such as input pressure, material thickness, and sensitivity. To maintain a constant voltage source, the piezo harvester output is connected to a capacitor unit. The

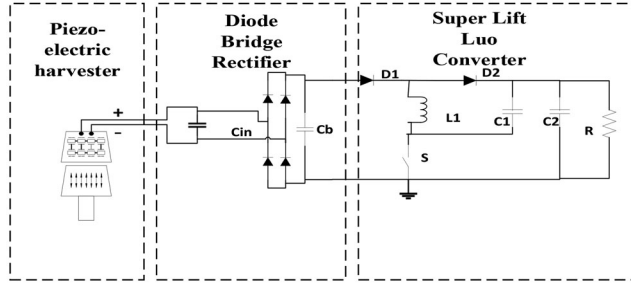


FIGURE 25. Open head frame with piezo harvester (4X2).

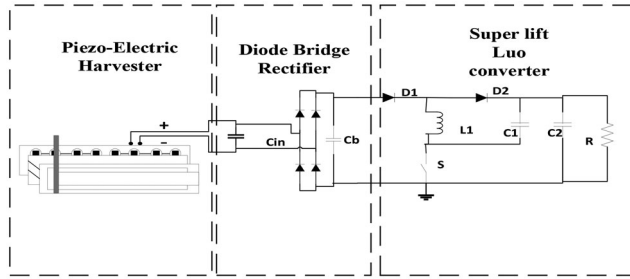


FIGURE 26. Open-end read with piezo harvester (2x10).

capacitor charges during the push and pull operations, and once it is fully charged, it discharges a constant voltage. This constant voltage is then forwarded to the uncontrolled diode bridge rectifier, which converts the AC power to uncontrolled DC power. However, uncontrolled DC power is not suitable for variable loads or battery energy storage units. Therefore, a super lift Luo converter with boosting mode DC-DC conversion is applied between the diode bridge rectifier and the load or energy storage unit. The super lift Luo converter helps reduce ripple content in the output voltage and current. It provides a high output voltage gain compared to other conventional DC-DC chopper circuits. The uncontrolled DC voltage from the diode bridge rectifier is applied to capacitor Cb, which maintains a constant input voltage source for the super lift Luo converter. The super lift Luo converter operates in two modes: power switch turn-on and power switch turn-off. During turn-on, capacitor 1 and inductor 1 charge, diode 2 is reverse biased, diode 1 is forward biased, and capacitor 2 circulates current to the load. During mode 2, capacitors charge, diode 2 turns on, diode 1 turns off, inductor 1 discharges, and the output current flows from inductor 1 and capacitor 1 to the load or energy storage unit. The parasitic element values of the super lift Luo converter are calculated using specific equations to ensure proper voltage gain and efficient operation.

$$\frac{V_o}{V_{in}} = \frac{(2 - K)}{(1 - K)} \quad (4)$$

$$K = \frac{2V_{in} - V_o}{V_o - V_{in}} \quad (5)$$

Inductor Value expression

$$L1 = \frac{V_o - 2V_{in}}{\Delta i l1} \frac{(1 - K)}{T} \quad (6)$$

Capacitor Value expression

$$C1,2 = \frac{(1 - K)}{f \Delta v_o} \frac{V_o}{R} \quad (7)$$

Based upon above equation capacitor and inductor value calculated.

4.4. Energy Estimation

In the energy estimation for the kinetic energy producers, specifically the X-Y open-end read and the vertical open-end head frame movable wooden pillar, the operational hours of the power loom are considered. Typically, single-shift power looms run for 8 to 9 h, although some large-scale industries may operate 24/7. For this project, an estimation of 1 h is taken into account, as it is more relevant for small-scale industries that typically have 1 or 2 power looms and work approximately 8 to 12 h. The energy estimation for the X-Y open-end read and the open-end head frame movable wooden pillar integrated with piezo plates is provided in Table 7 (Energy Estimation for Open-End Head Frame and Open-End Read-Based Electrokinetic Energy Extraction). For a single piezo cell, the minimum output voltage is 0.7 V AC, as shown in Figure 10 (Series-Parallel Piezo Plates V-I Characteristics). For the X-Y open-end read, a configuration of 3 × 3 piezo plates produce 7 V with 12 V AC. However, for the open-end head frame, the minimum output voltage is considered to be 0.7 V AC, as the weight of the wooden pillar is lower compared to the X-Y open-end read. The open-end read is typically made of steel, which results in a higher output voltage. However, for the purpose of estimation, a theoretical value of 2 V is considered.

5. EXPERIMENTAL SOURCE DETAILS ANALYSIS

The experimental setup for the extraction of electro-kinetic energy employs a matrix piezo array, as visualized in Figure 10 (Series Parallel Piezo Cell Connection). The

EKE particulars	Open end head frame	Open end read (X-Y shuttle)
Single Piezo cell	$V = 0.7V$ AC	$V = 2V$ AC
Single 4×2 Piezo Array Power	$P = VXI$ $P = 5.6 \times 0.012$ $P = 0.067W$	$P = VXI$ $P = 16 \times 0.012$ $P = 0.192W$
Energy Calculation per hour	$E = 0.448 \times 3600$ $E = 241.2$ Watts-hrs.	$E = 0.19 \times 3600$ $E = 691.2$ Watts-hrs.
Total number of EKE model presence	Single aluminum frame contains 3 Wooden pillar Totally 3 Frame so number of EKE is 9 $E = 9 \times 241.2$ $E = 2170.8$ Watts-hrs.	Single Read will integrate 2 (4×2) piezo arrays, totally 2 reads present so total of EKE model 4 $E = 4 \times 691.2$ $E = 2764.8$ Watts-hrs.

TABLE 7. Energy estimation for open end head frame and open end read based electro kinetic energy extraction.

piezo cells utilized in this setup feature a diameter of 27 mm and a thickness of 0.33 mm. These cells are interconnected in a series-parallel configuration, with each individual array comprising 8 piezo cells. Four sets of such piezo arrays are employed in the experiment. The arrays are incorporated within a wooden plate structure, as depicted in Figure 27 (Matrix Piezo Array Model for Open-End Head Frame), which facilitates the extraction of kinetic energy from the vertical movement of the open-end head frame. The interaction between a wooden pillar's up-and-down motion and the matrix piezo array is illustrated in Figure 28 (Wooden Pillar Force Applied Notations for Open-End Head Frame). This diagram elucidates how distinct sections of the array respond to the force exerted by the wooden pillar. Table 8 (Matrix Piezo Array Electrical Outputs due to Wooden Pillar Mass and Force) provides a comprehensive breakdown of the electrical outputs generated by the matrix piezo array, correlating them with the mass and force configurations of the wooden pillar. Notably, the open-end head frame-based matrix piezo array attains a maximum voltage output of 20 V, as showcased in Figure 29 (Matrix Piezo Array Output Voltage due to Wooden Pillar Object Moment). For the open-end X-Y read system, a configuration involving two matrix piezo arrays or ten piezo cells arranged in series (10×4 configuration) is adopted, as shown in Figure 30 (Matrix Piezo Array Model for Open-End X-Y Read). To safeguard the crystal structure from potential damage arising from direct force application by a steel object, the open-end read system integrates double-layer wooden and steel plates. Figure 31 (Double Layer Plates Force Applied Notation for Open-End X-Y Read) illustrates the force distribution across the double-layer wooden plates, serving as intermediaries between the read object and the piezo cells. Table 9 (Matrix Piezo Array Electrical Outputs due to Double

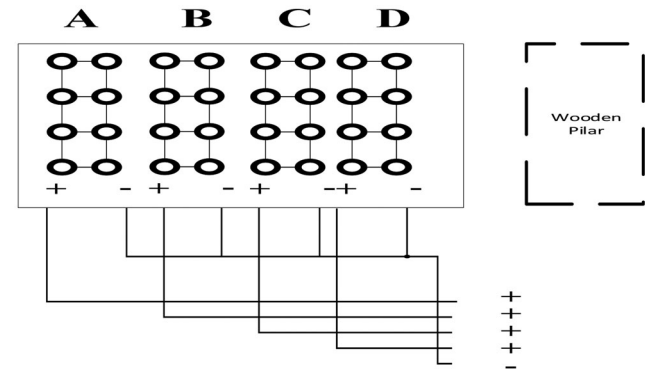


FIGURE 27. Matrix piezo array model for open end head frame.

Layer Wooden Pillar Mass and Force) further elaborates on the electrical output characteristics for the open-end X-Y read-based electro-kinetic energy conversion, considering the mass and force of the double-layer wooden object. In this context, the open-end read X-Y-based matrix piezo array achieves a maximum output voltage of 29.9 V, as demonstrated in Figure 32 (Matrix Piezo Array Output Voltage due to Double Layer Wooden Object Moment). Given that both the open-end head frame and open-end X-Y read-based electro-kinetic energy conversion models generate AC voltage due to the oscillatory nature of input kinetic energy, the AC voltage is inherently non-continuous and manifests as positive and negative half cycles. To rectify this AC voltage and ensure efficient energy extraction, separate half-wave rectifiers are integrated into both energy harvesting systems. A diode bridge rectifier and separate half-wave rectifiers (Da, Db, Dc, Dd) are employed. Figure 33 (Matrix Piezo Array Integration with Half-Wave Rectifier and Battery Energy Storage) illustrates the integration of the matrix piezo array with the half-wave

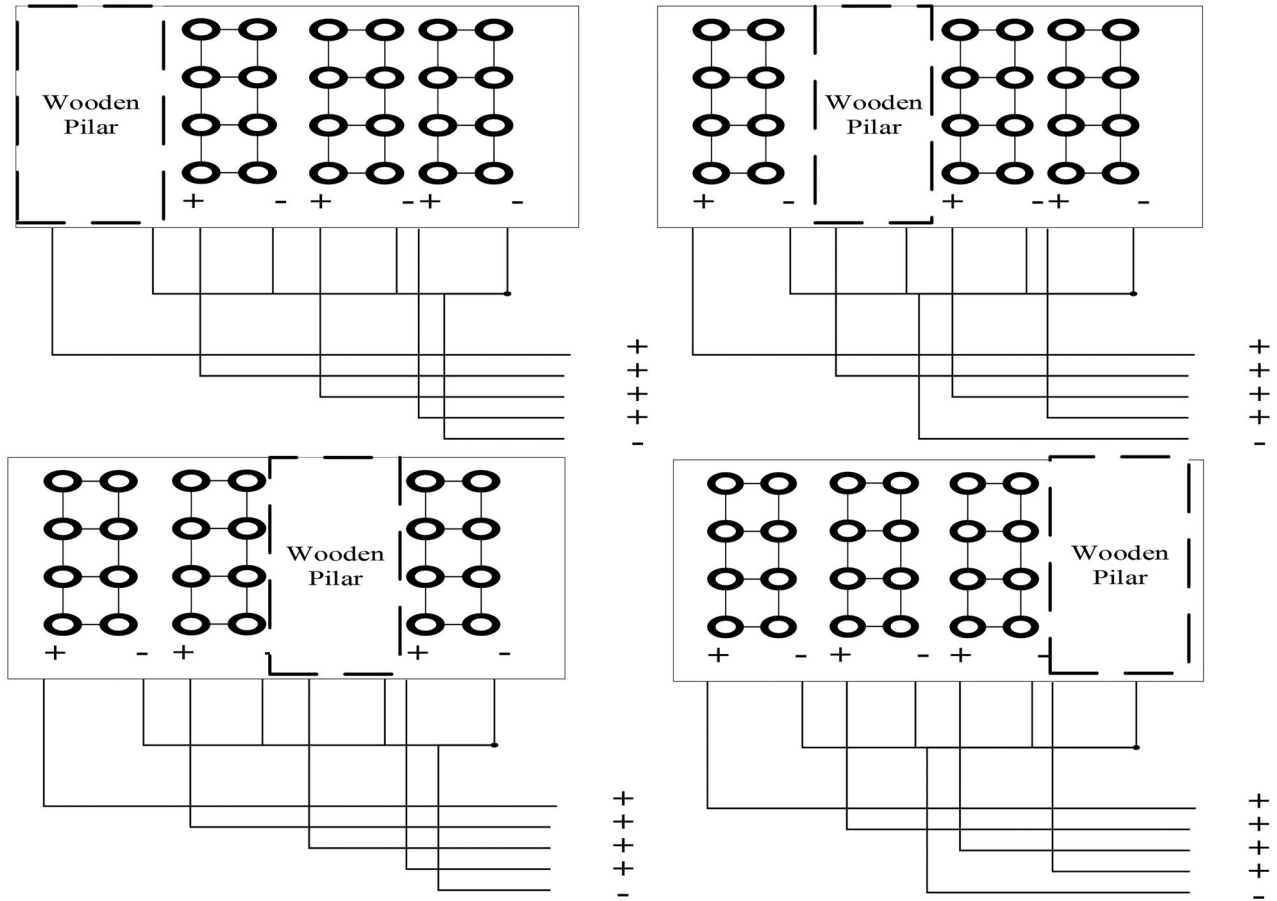


FIGURE 28. Wooden pillar force applied notations for open end head frame.

Matrix – Piezo Array Portion	Voltage(V)	Current (μ A)	Power(w)
A	20.01	0.010	0.20
A	21.23	0.011	0.23
B	17.76	0.012	0.21
B	19.89	0.012	0.23
C	21.10	0.010	0.24
C	20.12	0.012	0.24
D	20.34	0.011	0.22
D	18.87	0.010	0.18
Average	19.9	0.011	0.21

TABLE 8. Matrix piezo array electrical outputs due to wooden pillar mass and force.

rectifier and battery energy storage. The rectified DC voltage is temporarily stored in a capacitor (C_s), which charges during the electro-kinetic energy conversion process and discharges when fully charged. This capacitor is connected across a blocking diode to facilitate one-way energy flow from the source to the battery during forward bias. The setup includes two six-volt batteries connected in

series, resulting in a total voltage of 12 V, as depicted in Figure 34 (Battery Across Voltage). To achieve the second level of DC-DC power conversion, a positive output super lift Luo converter is employed, connected to the battery's output terminal. This converter operates in two modes: mode one involves the power switch turning on, allowing for the charging of inductor $L1$ and capacitor $C1$, while diode $D1$ becomes forward biased. In mode two, the power switch turns off, leading to capacitor $C2$'s discharge and the charging of capacitor $C1$, with diode $D2$ becoming forward biased. This configuration ensures a linear output voltage when the PWM signal is toggled on and off. Additionally, the reference voltage is extracted from the load terminal to optimize load operation. Figures 35 (Open-End Head Frame with Positive Output Super Lift Luo Converter) and 36 (Open-End X-Y Read with Positive Output Super Lift Luo Converter) visually illustrate these connections and operations.

The reference voltage is taken from the load terminal for efficient load operation. The reference voltage is forwarded to the voltage divider circuit; the divider will

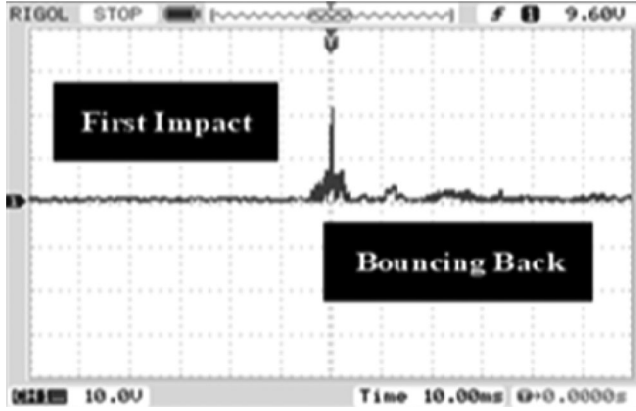


FIGURE 29. Matrix piezo array output voltage due to wooden pillar object moment.

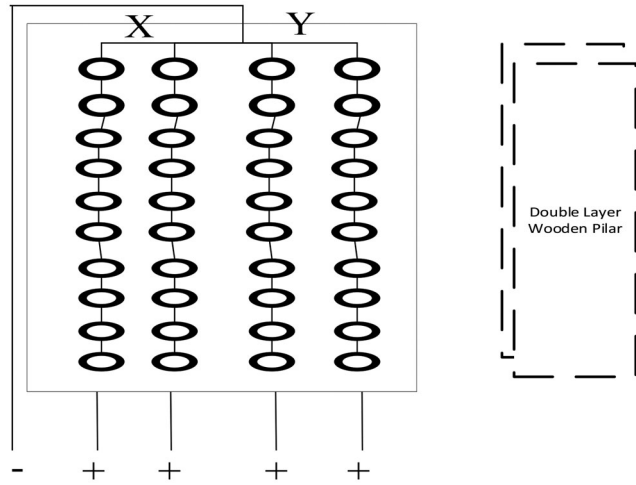


FIGURE 30. Matrix piezo array model for open end X-Y read.

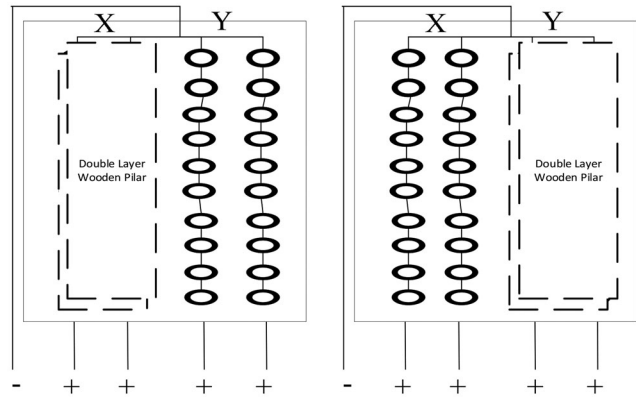


FIGURE 31. Double layer plates force applied notation for open end X-Y read.

divide the voltage based on the following equation:

$$V_{out} = \frac{R_2}{R_1 + R_2} \times V_{in} \quad (8)$$

The output voltage from the voltage divider circuit is directed to the controller, where the analog signal is read and subsequently converted into a digital signal. Within the controller, a digital condition block compares the reference voltage with the expected voltage. If these values align, the loop is broken; otherwise, corrective action through PWM signal adjustment occurs. This controller's operational sequence is meticulously outlined in the flowchart displayed in Figure 37 (Controller Action Flowchart). The corrected PWM signal is then transmitted to the push-pull driver circuit. This circuit serves the purpose of providing an isolated separate supply in conjunction with a ground-like isolation mechanism. The driver circuit triggers the main power switch of the Super Lift Luo converter. The PWM signal responsible for activating the power switch is illustrated in Figure 38 (PWM Signal for Power Switch). Figures 39 (Output Voltage of a Super Lift Luo Converter) and Figure 40 (Output Current of a Super Lift Luo Converter) visually showcase the resulting output voltage and current profiles of the Super Lift Luo converter, respectively. The voltage waveform is directly influenced by the divider output, which can be understood through Eq. (6). Conversely, the output current is gauged using a combination of shunt resistance and series load resistance. The voltage across the shunt resistance serves as a direct indicator of the output current's magnitude.

$$\mu A = \text{Voltage Across } R_h \times MF \quad (9)$$

if voltage increase across Shunt resistance means, output current also increases.

The detailed technical information about the circuit elements can be found in the following tables: Table 10 (Design Details about Half Wave Receptacle and Energy Storage Elements), Table 11 (Design Details about Super Lift Luo Converter), Table 12 (Details About Controller), and Table 13 (Details of Output Voltage and Current Waveforms). Additionally, Figure 41 (Controller Source Code) displays the Controller Source Code, which provides the source code details for the controller.

The experimental setup, depicted in Figure 42 (Hardware Model for Electro-Kinetic Energy Optimization), showcases the energy extraction unit and matrix piezo array structure specifically designed for the open-end head frame, as illustrated in Figure 35 (Open end Head Frame with Positive output super lift Luo converter)

Matrix – Piezo Array Portion	Voltage(V)	Current (μ A)	Power(w)
X	29.9	0.013	0.38
X	25.3	0.010	0.25
X	20.01	0.011	0.22
X	23.3	0.010	0.23
Y	25.8	0.010	0.25
Y	21.1	0.012	0.25
Y	27.3	0.011	0.30
Y	28.1	0.012	0.33
Average	25.35	0.011	0.27

TABLE 9. Matrix piezo array electrical outputs due to double layer wooden pillar mass and force.

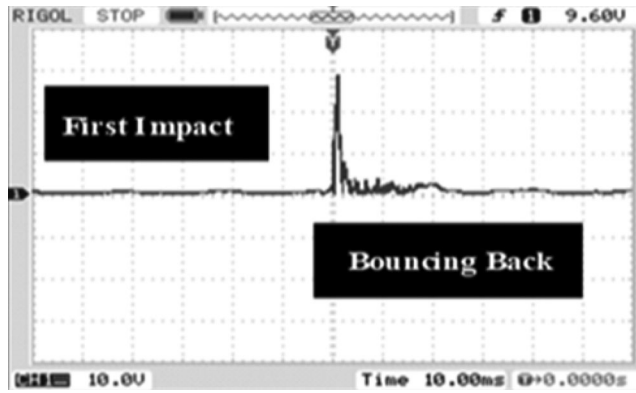


FIGURE 32. Matrix piezo array output voltage due to double layer wooden object moment.

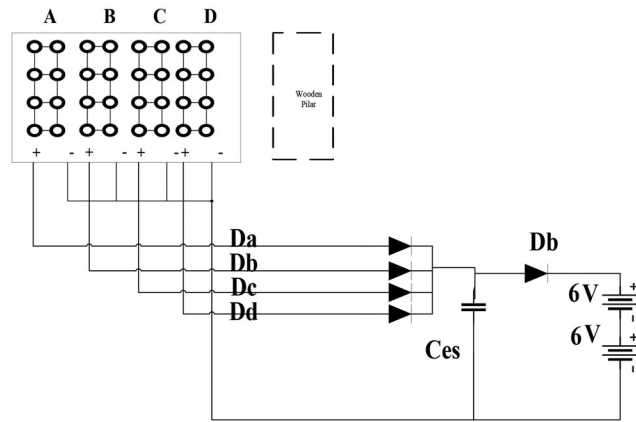


FIGURE 33. Matrix piezo array integration with half wave rectifier and battery energy storage.

and the open-end X-Y Read configuration shown in Figure 36 (Open-end X-Y Read with Positive output super lift Luo converter). However, the power electronics interface remains consistent across both setups.

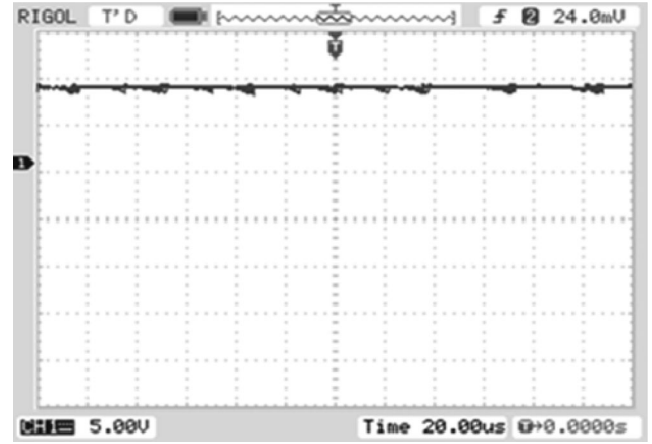


FIGURE 34. Battery across voltage.

6. ENERGY ESTIMATION VERIFICATION

The hardware model of the open-end head frame and open-end X-Y read-based electrokinetic energy extraction has been successfully validated in this research study. The experimental setup employed for energy estimation is presented in Table 14 (Energy Estimation based upon Hardware model), providing detailed insights into the energy estimation process based on the hardware model. The voltage and current measurements utilized in the estimation were obtained from Table 8 (1 Matrix Piezo array electrical outputs due to Wooden Pillar Mass and Force), which outlines the matrix piezo array's electrical outputs resulting from the wooden pillar mass and force, as well as from Table 9 (Matrix Piezo array electrical outputs due to double layer Wooden pillar Mass and Force), which depicts the matrix piezo array's electrical outputs due to the double layer wooden pillar mass and force. Through rigorous analysis, the average voltage and current values were calculated, demonstrating the effectiveness of the proposed electro-kinetic energy extraction models. These models hold significant relevance for electric drives employed in top closed loop and bottom closed loop power loom applications, where the extraction of electrical energy plays a pivotal role in their operation.

Theoretical energy estimation and practical energy estimation exhibited discrepancies primarily attributed to variations in kinetic energy and the material and configuration of the piezo array. However, both electro-kinetic energy extraction models effectively balance the power loom electric drive supply. According to existing literature, small-scale power loom industries typically require approximately 4 units of electricity per day, corresponding to an operational duration of 8 to 9 h. Based on the energy estimation

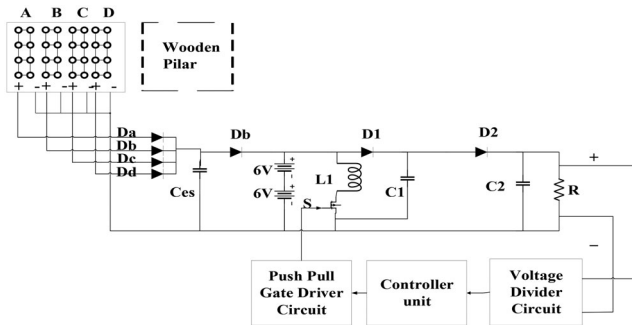


FIGURE 35. Open end head frame with positive output super lift luco converter.

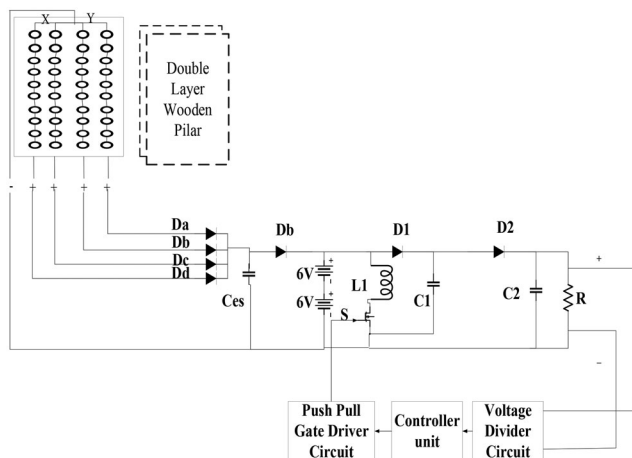


FIGURE 36. Open end X-Y read with positive output super lift Luo converter.

derived from our prototype models, the top closed loop power loom application can benefit from the open-end X-Y read-based electrokinetic energy extraction, while the bottom closed loop power loom can utilize the open head frame-based electro-kinetic energy extraction method.

Among the energy utilization methods discussed (Table 15 Comparative analysis of Electro-kinetic energy based weaving unit with Existing Power source based Weaving Unit), electro-kinetic energy stands out as a promising and innovative approach for optimizing energy utilization in weaving units. Its unique ability to continuously harness kinetic energy during the weaving process ensures a reliable and consistent power supply, independent of weather conditions, setting it apart from solar panels and wind turbines. Additionally, with a smaller footprint and relatively lower initial investments, electro-kinetic energy offers a cost-effective and scalable solution suitable for various weaving unit sizes and locations. In contrast, solar panels rely on capturing sunlight for electricity generation, making

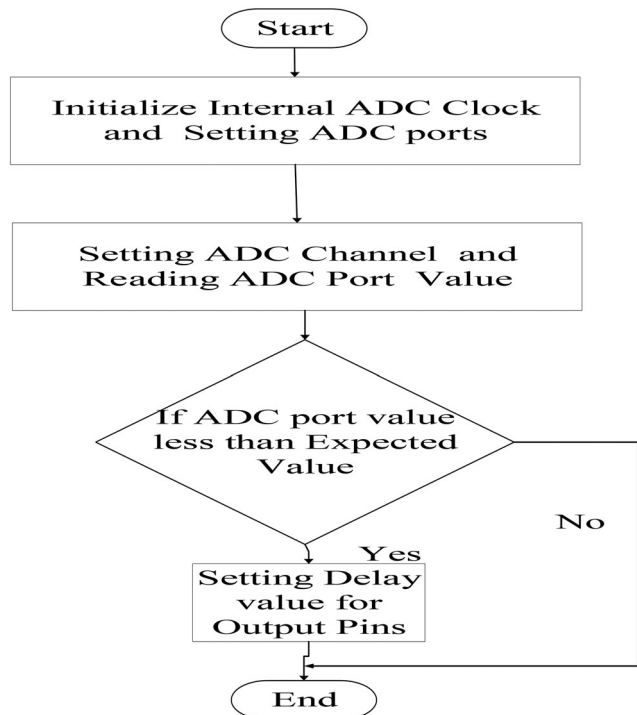


FIGURE 37. Controller action flowchart.

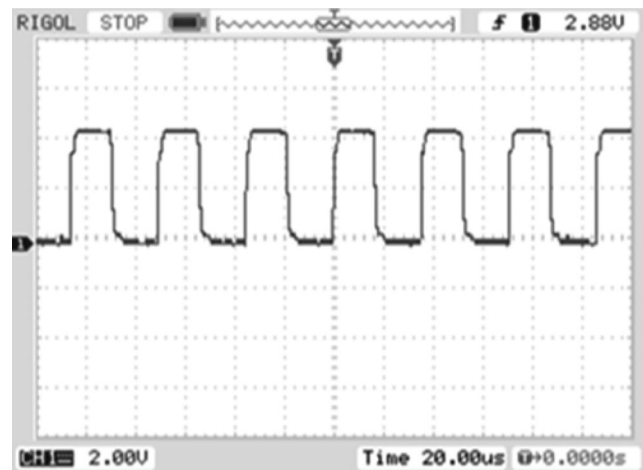


FIGURE 38. PWM signal for power switch.

them dependent on weather conditions such as cloud cover and daylight availability. Similarly, wind turbines rely on the presence of wind to generate electricity, making their energy output intermittent and influenced by wind patterns. Cogeneration, utilizing waste heat from power looms for electricity generation, provides an alternative to conventional energy sources. However, it may still rely on external electricity sources for stable power supply during periods of low waste heat availability. Electro-kinetic energy utilization presents a sustainable and independent

solution, continuously extracting kinetic energy during the weaving process and reducing the industry's environmental footprint. Its reliability, cost-effectiveness, and scalability make it a compelling choice for achieving a greener and more environmentally conscious future for the textile industry.

7. FUTURE SCOPE AND IMPLEMENTATION

The primary objective of this study is to enhance continuous energy extraction by devising closed-loop power loom-based electro-kinetic energy extraction models, both at the top and bottom levels. These models incorporate Matrix

Piezo arrays to enable efficient electro-kinetic energy conversion. Furthermore, alternative approaches, including open-wheel uni-directional non-linear energy extraction and linear power extraction from power loom-generated kinetic energy, are explored. The overarching aim is to decrease the dependence on gas and diesel-powered captive units in Medium and Large-scale power loom industries, where daily consumption averages around 4 units during 8–9 h of single power loom operation. The energy estimation derived from prototype models underscores that the top closed-loop power loom system can effectively leverage open-end X-Y read-based electro-kinetic energy extraction. On the other hand, the bottom closed-loop power loom system is better suited for open-head frame-based electro-kinetic energy extraction. These models offer promising avenues for optimizing energy supply within power loom operations, decreasing reliance on external power grids, and harnessing renewable energy sources like solar and micro wind turbines. An all-encompassing approach to indoor energy optimization within the industrial context involves all stages of electricity consumption across the industry. By tapping into power loom-free kinetic energy sources, energy harvesting can be streamlined, thereby minimizing transmission and distribution losses. However, continuous and efficient electro-kinetic energy extraction requires further refinements in the mechanical design of these energy extraction models. Future implementations might encompass additional electro-kinetic energy extraction sources, encompassing both linear and non-linear methods, to harness the kinetic energy inherent in power loom components. Such advancements aim to elevate energy levels harnessed from these extraction units. To affirm the stability and performance of all three electro-kinetic energy extraction models, the integration of machine learning algorithms can be beneficial, offering insights into

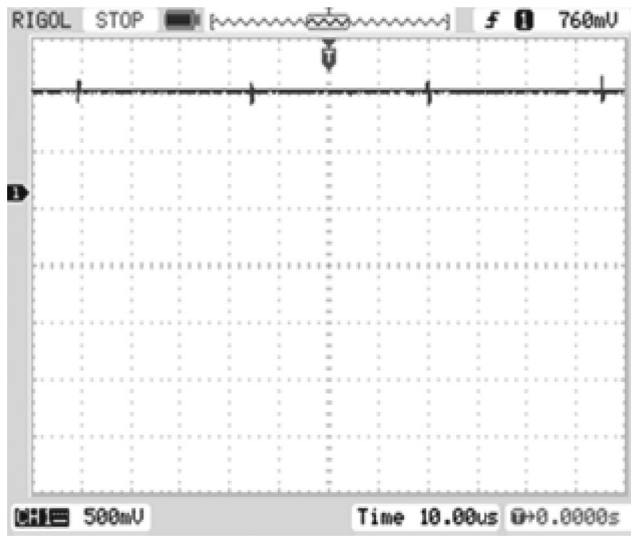


FIGURE 39. Output voltage of super lift Luo converter.

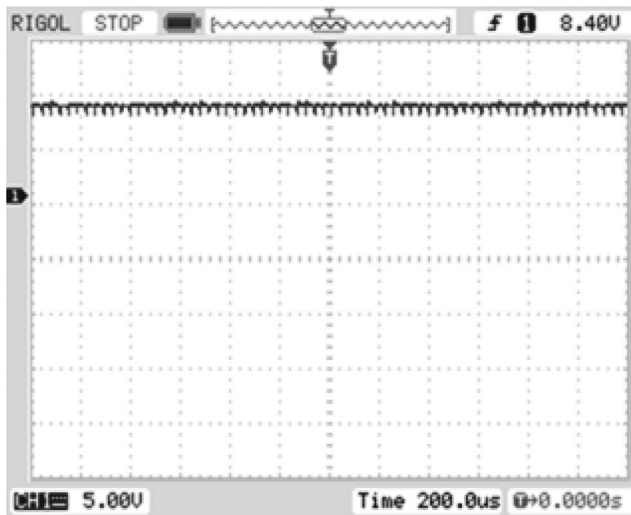


FIGURE 40. Output current of super lift Luo converter.

Half Wave Rectifier

Parameters	Ratings/Types	Data Sheet Id
Da, Db, Dc, Dd	0.3 V(FV)	UF4007
Ces	1000 μF , 25 V	–
Energy Storage Unit		
Battery	Two 6 Volt Lead Acid Type battery Amps per hour of battery is 5.5 amps	–

TABLE 10. Design details about half wave rectifier and energy storage elements.

$V_{in} = 12V$, $V_{out} = 100V$, $S_f = 20KHz$, $I_o = 0.85 A$

Power Equation	Theoretical Value	Practical Value
$\frac{V_o}{V_{in}} = \frac{(2-K)}{(1-K)}$	$K = 0.65$	$K = 0.5$
$I_o = \frac{V}{R}$	$R = 117 \text{ Ohm}$	$T_{on} = 20ms$ $T_{off} = 20ms$ $R = 100 \text{ ohm}$
$L1 = \frac{V_o - 2V_{in}}{\Delta i l1} \frac{(1-K)}{T}$	$\Delta i l1 = 0.1$ $L1 = 6mH$	$L1 = 4.5 \text{ mH}$
$C1,2 = \frac{(1-K)}{f \Delta v_o} \frac{V_o}{R}$	$\Delta V_o = 0.01$ $C1, C2 = 1495 \mu F$	$C1, C2 = 2200 \mu F$
$P_o = V_{out} \times I_{out}$	$P_o = 85 W$	$p = 85 W$
Parameters	Ratings /Types	Data Sheet Id
D1, D2	0.3 V(FV)	UF5408
Power Switch	N-Channel Mosfet	IRF450
Driver	Push pull Driver	BD140

TABLE 11. Design details about super lift luo converter.

Controller Type	Size of Controller	Data Sheet Id
PIC	8-bit Controller A0-PIN connected Voltage divider positive terminal, C1-PIN connected Push-pull driver Positive terminal	PIC16F887

TABLE 12. Details about controller.

their operational capabilities. As depicted in [Figure 43](#) (Typical Power Diagram of Future Implementation), a conceptual model illustrates three distinct electro-kinetic

energy extraction sources originating from power loom components, encompassing vertical, horizontal, and rotational kinetic energy. These sources incorporate components like lengthy open-wheel pipelines, yarn filing carrier pushers, X-Y read systems, and head frames. The power conversion process entails the use of a super lift Luo converter in the first stage, followed by advanced DC-DC power converters in subsequent stages, enhancing voltage gain and stability. In conclusion, this study significantly contributes to the optimization of continuous energy extraction in power loom applications through the development of sophisticated electro-kinetic energy extraction models. The findings underscore the potential to lessen reliance on conventional power sources, utilize renewable energy, and stress the importance of refining mechanical designs and

Wave form type	Calculation	Value
Voltage	Output Voltage $V_o = \frac{R2}{R1 + R2} \times V_{in}$ $R1 = 100 \text{ ohm}$ $R2 = 1 \text{ ohm}$ $V_{in} = 100$	If 100 V output voltage means DSO show $V_o = 1 V$
Voltage	Feed Back Voltage for Controller $V_o = \frac{R2}{R1 + R2} \times V_{in}$ $R1 = 100 \text{ ohm}$ $R2 = 5 \text{ ohm}$ $V_{in} = 100 V$	If 100 V output voltage means Feed Back voltage is $V_o = 5 V$
Current	Output Current $\mu A = V_{Rsh} \times MF$ $V_{Rsh} = 8.4$ $MF = 100$	$A = 0.8 A$

TABLE 13. Details of output voltage and current wave forms.


```
#include <16f887.h>
#fuses INTRC_IO, NOWDT, NOPUT, NOBROWNOUT, NOMCLR,
PROTECT
#device adc=10
#use delay(clock=4M)
int i=0;
void main()
{
    setup_adc(ADC_CLOCK_INTERNAL); // initialize ADC with a sampling
    rate of Crystal/4 MHz
    setup_adc_ports(sAN0,sAN1);
    while(1)
    {
        for(i=0;i<100;i++)
        {
            output_high(pin_c1);
            delay_us(12);
            output_low(pin_c1);
            delay_us(8);
        }
        set_adc_channel(0);
        delay_us(1);
        int c1 = read_adc();
        delay_us(1);
        if(c1<255)
        {
            output_high(pin_c1);
            delay_us(12);
            output_low(pin_c1);
            delay_us(8);
        }
        else
        {
            output_low(pin_c1);
        }
    }
}
```

FIGURE 41. Controller source code.

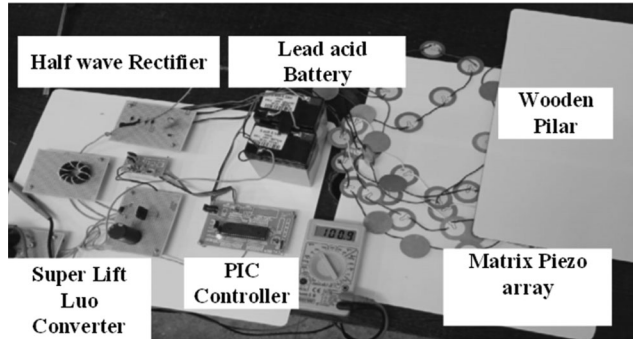


FIGURE 42. Hardware model for electro-kinetic energy extraction.

embracing future advancements in the field of electro-kinetic energy extraction.

8. CONCLUSION

In conclusion, this project is driven by the goal to revolutionize energy utilization in the textile industry through the enhancement of Modified Piezo Matrix-based electro-kinetic energy generation from weaving power looms. By focusing on tapping into two distinct sources of kinetic energy – the open-end head frame and the Weaving X-Y Shuttle box – the project aims to continuously harness electrical energy that is otherwise wasted during the weaving process. The experimental setup, featuring advanced piezo matrices with specific wooden actions, effectively captures and converts sequential kinetic energy into usable electrical power. The quantified energy estimation demonstrates the significant potential of this approach, with the Open end Head frame model yielding 9.51 Hp and the Weaving X-Y Shuttle box generating 2.60 Hp. To enhance energy savings and integration within the industrial context, a second-level DC-DC power conversion using the Super Lift Luo converter is implemented. This not only ensures optimal power transfer but also facilitates integration with the Industrial DC microgrid, contributing to efficient energy utilization. The project's overarching objectives encompass optimizing energy consumption, reducing reliance on fossil fuels, and championing sustainability within the textile industry. The approach emphasizes the utilization of otherwise wasted kinetic energy, the optimization of energy usage, and the showcase of electrokinetic solutions' immense potential. By seeking to transform the energy landscape of the textile industry, this project strives to catalyze a shift toward sustainable and environmentally conscious production practices. Through the convergence of innovative technologies, efficient energy utilization, and

EKE particulars	Open end head frame	Open end read (X-Y Shuttle)
Average Voltage and Current	$V = 19.9V$ $I = 0.011 A$	$V = 25.35V$ $I = 0.011 A$
Single Piezo Array Power	$P = VXI$ $P = 19.9 \times 0.011$ $P = 0.2189W$	$P = VXI$ $P = 25.3 \times 0.011$ $P = 0.27W$
Energy Calculation per hour	$E = 0.2189 \times 3600$ $E = 788.04 \text{ Watts-hrs.}$	$E = 0.19 \times 3600$ $E = 972 \text{ Watts-hrs.}$
Total number of EKE model presence	Single aluminum frame contains 3 Wooden pillar Totally 3 Frame so number of EKE is 9 $E = 9 \times 788.04$ $E = 7092.36 \text{ Watts-hrs or } 9.51 \text{ HP}$	Single Read will integrate (10×2) piezo arrays, totally 2 reads present so total of EKE model 2 $E = 2 \times 972$ $E = 1944 \text{ Watts-hrs or } 2.60 \text{ HP}$

TABLE 14. Energy estimation based upon hardware model.

Parameter	Solar and Wind-Based Energy Utilization in Weaving Units	Co-Generation Based Energy Utilization in Weaving Units	Electro-Kinetic Energy Based Energy Utilization in Weaving Units
Reliability	Affected by weather conditions and wind availability	Relies on waste heat availability from power looms	Not affected by weather conditions, continuous energy extraction
Energy Storage	Requires energy storage for use during non-sunny and low wind periods	May require energy storage for consistent electricity supply	Continuous energy extraction, no need for additional storage
Initial Investment	High initial investment for solar panel and wind turbine installation	Requires initial investment for cogeneration equipment	Lower initial investment for piezoelectric element implementation
Space Requirement	Requires sufficient open space for solar panel and wind turbine installation	Requires space for cogeneration equipment	Requires a well-designed mechanical structure with a smaller footprint
Environmental Impact	Renewable energy source, reduces carbon footprint	Reduces carbon emissions by utilizing waste heat for electricity	Renewable energy source, reduces carbon footprint
Scalability	Can be scaled up with additional solar panels and wind turbines	Scalable for different sizes of power looms	Scalable for different sizes of weaving units
Energy Independence	Can reduce dependence on external power sources	Reduces dependence on external electricity sources	Provides a degree of energy independence and reduces reliance on conventional energy sources
Maintenance	Requires regular cleaning and maintenance	Requires maintenance of cogeneration equipment	Lower maintenance, mainly related to mechanical components
Efficiency	Efficiency varies based on sunlight and wind availability	Efficiency depends on waste heat utilization	Efficiency depends on the design and optimization of the electrokinetic system
Application Flexibility	Suitable for regions with ample sunlight and consistent wind patterns	Suitable for power looms with waste heat generation	Suitable for various locations, not dependent on specific weather patterns
Environmental Footprint	Requires land use for solar panel and wind turbine installation	Reduces environmental footprint by utilizing waste heat for electricity	Minimal environmental footprint, primarily utilizes wasted kinetic energy

TABLE 15. Comparative analysis of electro-kinetic energy based weaving unit with existing power source based weaving unit.

a commitment to reducing the industry's ecological footprint, the project serves as a beacon of change that has the potential to reshape energy consumption norms within the textile sector. Ultimately, its success could pave the way for a more sustainable future for the industry, aligning energy efficiency with environmental responsibility.

9. FUTURE WORKS FOR ELECTRO-KINETIC SOLUTIONS

This research holds immense importance for the World Scientific Community as it addresses crucial challenges in the field of energy optimization and sustainability. By

investigating and harnessing the potential of electro-kinetic energy extraction, this work offers a greenhouse gas-free and environmentally friendly method for energy harvesting. The significance of this research lies in its potential to revolutionize industrial energy consumption. Traditional energy sources, often reliant on fossil fuels, contribute to environmental pollution and climate change. By promoting the use of electro-kinetic energy extraction, industries can significantly reduce their carbon footprint and transition toward greener energy practices. Moreover, the affordability and low technical complexity of electro-kinetic energy extraction make it accessible to various industries, regardless of their scale of operation. This inclusivity ensures

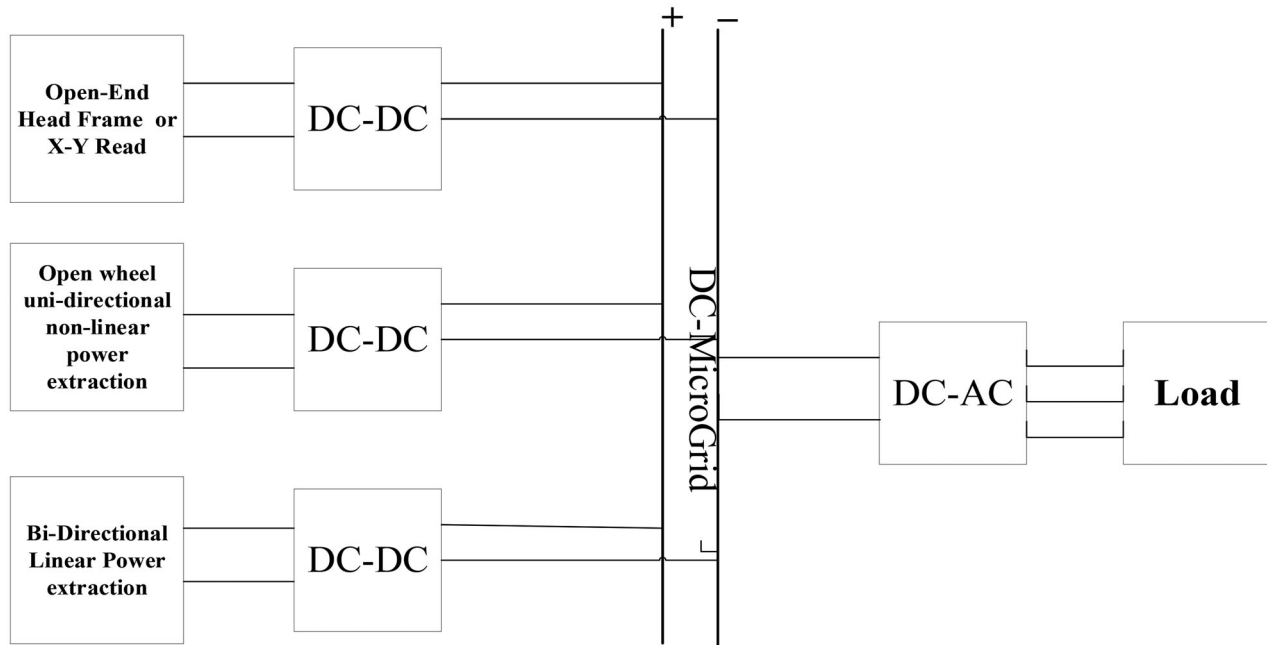


FIGURE 43. Typical power diagram of future implementation.

that a wide range of sectors can benefit from sustainable energy solutions, leading to a positive impact on global energy consumption patterns. The potential integration of renewable energy sources and energy storage technologies further enhances the value of this research. By combining these technologies with electro-kinetic solutions, a more stable and reliable energy supply can be achieved, contributing to a more resilient and sustainable energy infrastructure. Furthermore, the incorporation of advanced control and optimization algorithms demonstrates the cutting-edge approach of this research. By leveraging machine learning and artificial intelligence techniques, energy harvesting and utilization can be optimized to maximize efficiency and energy savings. Overall, this research project serves as a pioneering initiative in advancing sustainable energy practices and promoting a greener future for industries worldwide. Its potential for practical implementation and real-world impact makes it a valuable contribution to the World Scientific Community's ongoing efforts toward a sustainable and eco-friendly world.

DISCLOSURE STATEMENT

No potential conflict of interest was reported by the author(s).

REFERENCES

- [1] A. Çay, "Energy consumption and energy saving potential in clothing industry," *Energy*, vol. 159, pp. 74–85, 2018. DOI: [10.1016/j.energy.2018.06.128](https://doi.org/10.1016/j.energy.2018.06.128).
- [2] L. Peng *et al.*, "Energy efficiency and influencing factor analysis in the overall Chinese textile industry," *Energy*, vol. 93, pp. 1222–1229, 2015. DOI: [10.1016/j.energy.2015.09.075](https://doi.org/10.1016/j.energy.2015.09.075).
- [3] L. Zhang, M. Y. Leung, S. Boriskina, and X. Tao, "Advancing life cycle sustainability of textiles through technological innovations," *Nat. Sustain.*, vol. 6, no. 3, pp. 243–253, 2023. DOI: [10.1038/s41893-022-01004-5](https://doi.org/10.1038/s41893-022-01004-5).
- [4] "Manual on Energy Conservation in Textile Cluster," 2019.
- [5] V. Santhosh and K. Poorna, "A study on electricity problem in powerloom units (special reference with Coimbatore District)," *Paripex-Indian J. Res.*, vol. 11, pp. 30–31, 2014.
- [6] Y. Dhayaneswaran and L. Ashokkumar, "A study on energy conservation in textile industry," *J. Inst. Eng. India Ser. B*, vol. 94, no. 1, pp. 53–60, 2013. DOI: [10.1007/s40031-013-0040-5](https://doi.org/10.1007/s40031-013-0040-5).
- [7] M. Safaei, H. A. Sodano and S. R. Anton, "A review of energy harvesting using piezoelectric materials: state-of-the-art a decade later (2008–2018)," *Smart Mater. Struct.*, vol. 28, no. 11, pp. 113001, 2019. DOI: [10.1088/1361-665X/ab36e4](https://doi.org/10.1088/1361-665X/ab36e4).
- [8] A. Hasanbeigi, "Energy-efficiency improvement opportunities for the textile industry," no LBNL-3970E, Lawrence Berkeley National Lab (LBNL), Berkeley, CA United States, 2010. DOI: [10.2172/991751](https://doi.org/10.2172/991751).
- [9] Van Dongen, Pauline, Ellen Britton, Anna Wetzel, Rogier Houtman, Ahmed Mohamed Ahmed, and Stephanie Ramos, "Suntex: weaving solar energy into building skin," *J.*

- Facade Des. Eng.*, vol. 10, no. 2, pp. 141–160, 2022. DOI: [10.47982/jfde.2022.powerskin.9](https://doi.org/10.47982/jfde.2022.powerskin.9).
- [10] H. Toshiyoshi *et al.*, “MEMS vibrational energy harvesters,” *Sci. Technol. Adv. Mater.*, vol. 20, no. 1, pp. 124–143, 2019. DOI: [10.1080/14686996.2019.1569828](https://doi.org/10.1080/14686996.2019.1569828).
- [11] D. Gielen *et al.*, “The role of renewable energy in the global energy transformation,” *Energy Strategy Rev.*, vol. 24, pp. 38–50, 2019. DOI: [10.1016/j.esr.2019.01.006](https://doi.org/10.1016/j.esr.2019.01.006).
- [12] M. R. Sarker *et al.*, “Review of piezoelectric energy harvesting system and application of optimization techniques to enhance the performance of the harvesting system,” *Sensors Actuators A: Phys.*, vol. 300, pp. 111634, 2019. DOI: [10.1016/j.sna.2019.111634](https://doi.org/10.1016/j.sna.2019.111634).
- [13] S. Naik and V. Bagodi, “Energy conservation opportunities: evidences from three industrial clusters in India,” *IJESM*, vol. 15, no. 3, pp. 600–627, 2021. DOI: [10.1108/IJESM-07-2020-0022](https://doi.org/10.1108/IJESM-07-2020-0022).
- [14] P. Khude, “A review on energy management in textile industry,” *Innov. Ener. Res.*, vol. 06, no. 02, pp. 169, 2017. DOI: [10.4172/2576-1463.1000169](https://doi.org/10.4172/2576-1463.1000169).
- [15] E. Ozturk *et al.*, “Improving energy efficiency using the most appropriate techniques in an integrated woolen textile facility,” *J. Cleaner Prod.*, vol. 254, pp. 120145, 2020. DOI: [10.1016/j.jclepro.2020.120145](https://doi.org/10.1016/j.jclepro.2020.120145).
- [16] B. Dudem, D. H. Kim, and J. S. Yu, “Triboelectric nanogenerators with gold-thin-film-coated conductive textile as floating electrode for scavenging wind energy,” *Nano Res.*, vol. 11, no. 1, pp. 101–113, 2018. DOI: [10.1016/j.apenergy.2018.09.009](https://doi.org/10.1016/j.apenergy.2018.09.009).
- [17] S. Z. Jia, “Waste energy harvesting in sustainable manufacturing,” *Sustain. Manuf. Process.*, pp. 231–256, 2023. DOI: [10.1016/B978-0-323-99990-8.00014-X](https://doi.org/10.1016/B978-0-323-99990-8.00014-X).
- [18] Z. Hadas, L. Janak, and J. Smilek, “Virtual prototypes of energy harvesting systems for industrial applications,” *Mech. Syst. Signal Process.*, vol. 110, pp. 152–164, 2018. DOI: [10.1016/j.ymssp.2018.03.036](https://doi.org/10.1016/j.ymssp.2018.03.036).
- [19] M. J. Burke and J. C. Stephens, “Political power and renewable energy futures: a critical review,” *Energy Res. Social Sci.*, vol. 35, pp. 78–93, 2018. DOI: [10.1016/j.erss.2017.10.018](https://doi.org/10.1016/j.erss.2017.10.018).
- [20] J. R. Albert, K. Ramasamy, V. Joseph Michael Jerard, R. Boddepalli, G. Singaram, and A. Loganathan, “A symmetric solar photovoltaic inverter to improve power quality using digital pulsewidth modulation approach,” *Wireless Pers. Commun.*, vol. 130, no. 3, pp. 2059–2097, 2023. DOI: [10.1007/s11277-023-10372-w](https://doi.org/10.1007/s11277-023-10372-w).
- [21] S. Hemalatha, A. Johny Renoald, G. Banu, and K. Indirajith, “Design and investigation of PV string/central architecture for bayesian fusion technique using grey wolf optimization and flower pollination optimized algorithm,” *Energy Conversion Manage.*, vol. 286, pp. 117078, 2023. DOI: [10.1016/j.enconman.2023.117078](https://doi.org/10.1016/j.enconman.2023.117078).
- [22] P. K. Pathak, A. K. Yadav, S. Padmanaban, and P. A. Alvi, “Design of robust multi-rating battery charger for charging station of electric vehicles via solar PV system,” *Electric Power Components Syst.*, vol. 50, no. 14–15, pp. 751–761, 2022. DOI: [10.1080/15325008.2022.2139870](https://doi.org/10.1080/15325008.2022.2139870).
- [23] J. R. Albert *et al.*, “Investigation on load harmonic reduction through solar-power utilization in intermittent SSFI using particle swarm, genetic, and modified firefly optimization algorithms,” *IFS*, vol. 42, no. 4, pp. 4117–4133, 2022. DOI: [10.3233/JIFS-212559](https://doi.org/10.3233/JIFS-212559).
- [24] A. D. Woldeyohannes, D. E. Woldemichael, and A. T. Baheta, “Sustainable renewable energy resources utilization in rural areas,” *Renew. Sustain. Energ. Rev.*, vol. 66, pp. 1–9, 2016. DOI: [10.1016/j.rser.2016.07.013](https://doi.org/10.1016/j.rser.2016.07.013).
- [25] H. Haes Alhelou, M. E. Hamedani Golshan, and M. Hajiakbari Fini, “Wind driven optimization algorithm application to load frequency control in interconnected power systems considering GRC and GDB nonlinearities,” *Electric Power Compon. Syst.*, vol. 46, no. 11–12, pp. 1223–1238, 2018. DOI: [10.1080/15325008.2018.1488895](https://doi.org/10.1080/15325008.2018.1488895).
- [26] C. Gnanavel, P. Muruganantham, and K. Vanchinathan, “Experimental validation and integration of solar PV fed modular multilevel inverter (MMI) and flywheel storage system,” 2021 IEEE Mysore Sub Section International Conference (MysuruCon), pp. 147–153, IEEE. DOI: [10.1109/MysuruCon52639.2021.9641650](https://doi.org/10.1109/MysuruCon52639.2021.9641650).
- [27] J. R. Albert and A. A. Stonier, “Design and development of symmetrical super-lift DC–AC converter using firefly algorithm for solar-photovoltaic applications,” *IET Circuits, Devices & Syst.*, vol. 14, no. 3, pp. 261–269, 2020. DOI: [10.1049/iet-cds.2018.5292](https://doi.org/10.1049/iet-cds.2018.5292).
- [28] J. R. Albert, A. A. Stonier, and K. Vanchinathan, “Testing and performance evaluation of water pump irrigation system using voltage-lift multilevel inverter,” *Int. J. Ambient Energy*, vol. 43, no. 1, pp. 8162–8175, 2022. DOI: [10.1080/01430750.2022.2092773](https://doi.org/10.1080/01430750.2022.2092773).
- [29] L. Thangamuthu, J. R. Albert, K. Chinnanan, and B. Gnanavel, “Design and development of extract maximum power from single-double diode PV model for different environmental condition using BAT optimization algorithm,” *IFS*, vol. 43, no. 1, pp. 1091–1102, 2022. DOI: [10.3233/JIFS-213241](https://doi.org/10.3233/JIFS-213241).
- [30] S. Impram *et al.*, “Challenges of renewable energy penetration on power system flexibility: a survey,” *Energy Strategy Rev.*, vol. 31, pp. 100539, 2020. DOI: [10.1016/j.esr.2020.100539](https://doi.org/10.1016/j.esr.2020.100539).
- [31] S. Ould Amrouche, Djamila Rekioua, Toufik Rekioua, and Seddik Bacha, “Overview of energy storage in renewable energy systems,” *Int. J. Hydro. Energ.*, vol. 41, no. 45, pp. 20914–20927, 2016. DOI: [10.1016/j.ijhydene.2016.06.243](https://doi.org/10.1016/j.ijhydene.2016.06.243).
- [32] P. K. Pathak and A. K. Yadav, “Design of battery charging circuit through intelligent MPPT using SPV system,” *Solar Energy*, vol. 178, pp. 79–89, 2019. DOI: [10.1016/j.solener.2018.12.018](https://doi.org/10.1016/j.solener.2018.12.018).
- [33] D. Li, S. Zhang, and Y. Xiao, “Interval optimization-based optimal design of distributed energy resource systems under uncertainties,” *Energies*, vol. 13, no. 13, pp. 3465, 2020. DOI: [10.3390/en13133465](https://doi.org/10.3390/en13133465).
- [34] R. Haas *et al.*, “The looming revolution: how photovoltaics will change electricity markets in Europe fundamentally,” *Energy*, vol. 57, pp. 38–43, 2013. DOI: [10.1016/j.energy.2013.04.034](https://doi.org/10.1016/j.energy.2013.04.034).

- [35] A. Hasanbeigi and L. Price, "A review of energy use and energy efficiency technologies for the textile industry," *Renew. Sustain. Energy Rev.*, vol. 16, no. 6, pp. 3648–3665, 2012. DOI: [10.1016/j.rser.2012.03.029](https://doi.org/10.1016/j.rser.2012.03.029).
- [36] A. Aabid *et al.*, "Systematic review of piezoelectric materials and energy harvesters for industrial applications," *Sensors*, vol. 21, no. 12, pp. 4145, 2021. DOI: [10.3390/s21124145](https://doi.org/10.3390/s21124145).
- [37] N. A. Abidin, "The simulation analysis of piezoelectric transducer with multi-array configuration," *J. Phy.*, vol. 1, pp. 012042, 2020. DOI: [10.1088/1742-6596/1432/1/012042](https://doi.org/10.1088/1742-6596/1432/1/012042).
- [38] G. D. Ramady, A. Anung, M. S. Sungkar, Y. A. Nugraha, and A. Wirjawan, "Reduksi Rugi-Rugi Pensaklaran Pada Konverter Dc-Dc Zeta Dengan Teknik Zero Voltage Transition," *Power Elektronik: Jurnal Orang Elektro.*, vol. 12, no. 1, pp. 49–53, 2023. DOI: [10.30591/polektro.v12i1.4378](https://doi.org/10.30591/polektro.v12i1.4378).
- [39] Y. Liang and S. Lin, "Research on bi-directional four-port converter of solar electric vehicle," *Energy Rep.*, vol. 9, pp. 271–278, 2023. DOI: [10.1016/j.egy.2022.12.125](https://doi.org/10.1016/j.egy.2022.12.125).
- [40] H. Al-Baidhani and M. K. Kazimierzuk, "Simplified non-linear current-mode control of DC-DC cuk converter for low-cost industrial applications," *Sensors*, vol. 23, no. 3, pp. 1462, 2023. DOI: [10.3390/s23031462](https://doi.org/10.3390/s23031462).
- [41] P. K. Pathak, A. K. Yadav, S. Padmanaban, P. A. Alvi, and I. Kamwa, "Fuel cell-based topologies and multi-input DC–DC power converters for hybrid electric vehicles: a comprehensive review," *IET Generation Trans. Dist.*, vol. 16, no. 11, pp. 2111–2139, 2022. DOI: [10.1049/gtd2.12439](https://doi.org/10.1049/gtd2.12439).
- [42] K. Gurumoorthy and S. Balaraman, "Controlling the speed of renewable-sourced DC drives with a series compensated DC to DC converter and sliding mode controller," *Automatika*, vol. 64, no. 1, pp. 114–126, 2023. DOI: [10.1080/00051144.2022.2118099](https://doi.org/10.1080/00051144.2022.2118099).
- [43] P. Nagaveni, M. Siva RamKumar, M. Nivetha, A. Amudha, and G. Emayavaramban, "Electrical energy audit – an experience in a small scale textile mill," *Int. J. Innov. Technol. Explor. Eng.*, vol. 8, no. 10, pp. 4102–4107, 2019. DOI: [10.1016/j.jclepro.2010.01.006](https://doi.org/10.1016/j.jclepro.2010.01.006).
- [44] R. Velmurugan and K. P. Balraj, "Recent issues and challenges of weaving industry with special reference to select Taminadu districts," *Int. J. Sci. Advance Res. Technol.*, vol. 4, no. 1, pp. 510–512, 2018.
- [45] R. Arulmozhiyal and K. Baskaran, "Implementation of a fuzzy PI controller for speed control of induction motors using FPGA," *J. Power Electronics*, vol. 10, no. 1, pp. 65–71, 2010. DOI: [10.6113/JPE.2010.10.1.065](https://doi.org/10.6113/JPE.2010.10.1.065).
- [46] M. Mahmoud *et al.*, "A review of mechanical energy storage systems combined with wind and solar applications," *Energy Conversion Manage.*, vol. 210, pp. 112670, 2020. DOI: [10.1016/j.enconman.2020.112670](https://doi.org/10.1016/j.enconman.2020.112670).
- [47] Kaniz Farhana, Kumaran Kadirgama, Abu Shadate Faisal Mahamude, and Mushfika Tasnim Mica, "Energy consumption, environmental impact, and implementation of renewable energy resources in global textile industries: an overview towards circularity and sustainability," *Mater. Circ. Econ.*, vol. 4, no. 1, p. 15, 2022.
- [48] S. G. Kim, S. Priya, and I. Kanno, "Piezoelectric MEMS for energy harvesting," *MRS Bull.*, vol. 37, no. 11, pp. 1039–1050, 2012. DOI: [10.1088/1742-6596/660/1/012001](https://doi.org/10.1088/1742-6596/660/1/012001).
- [49] G. D. Szarka, B. H. Stark, and S. G. Burrow, "Review of power conditioning for kinetic energy harvesting systems," *IEEE Trans. Power Electron.*, vol. 27, no. 2, pp. 803–815, 2012. DOI: [10.1109/TPEL.2011.2161675](https://doi.org/10.1109/TPEL.2011.2161675).

BIOGRAPHIES

Karthikeyan Saravanan is a Ph.D. candidate at Anna University, where he is currently pursuing his doctoral research. Karthikeyan is a dedicated and prolific researcher, having already published 11 research papers in prestigious international journals, demonstrating his commitment to contributing valuable insights to these areas of study. His academic journey and research endeavours highlight his passion for advancing knowledge and technology in the field of electrical engineering. His research is centered on the optimization of electrokinetic energy in indoor industrial units, reflecting his deep interest in the field of power electronics, drives, and renewable power sources.

Johny Renoald Albert, Ph.D., is an experienced academic and researcher specializing in power electronics and renewable energy. Holding a Ph.D. from Anna University, Chennai, and prior degrees in Electrical & Electronics Engineering, he has 12 years of teaching experience and nearly five years of research expertise. With a background that includes an industrial stint at M.P.S Steels Pvt. Ltd., he now serves as an Assistant Professor at Erode Sengunthar Engineering College (Autonomous), focusing on power system analysis, power quality issues, and renewable energy resources. Dr. Albert has an impressive publication record with numerous papers in SCI and Scopus-indexed journals, and he is a respected reviewer for prominent publishers like IEEE, Springer, Elsevier, IET, IOS, and Wiley.